A MASTER'S THESIS

Functional Investigation of *ACCELERATED CELL DEATH 6* in Shaping Natural Diversity of Age- and Salicylic Acid-Induced Leaf Senescence in Arabidopsis

Nguyen Nguyen Chuong

Department of Interdisciplinary Graduate Program in Advanced Convergence Technology and Science
GRADUATE SCHOOL
JEJU NATIONAL UNIVERSITY

February 2024

Functional Investigation of *ACCELERATED CELL DEATH 6* in Shaping Natural Diversity of Age- and Salicylic Acid-Induced Leaf Senescence in Arabidopsis

Nguyen Nguyen Chuong

(Supervised by Professor Kim Jeongsik)

A thesis submitted in partial fulfillment of the requirement for the degree of Master of Interdisciplinary Graduate Program in Advanced Convergence Technology and Science

2023. 12. 08

This thesis has been examined and approved.

Jin Hee Kim

Thesis director, Jin Hee Kim, Research Professor of Subtropical Horticulture Research Institute, Jeju National University

Hong-Gyu KANG

Hong-Gyu Kang, Research Professor of Subtropical Horticulture Research Institute, Jeju National University

Jeongsik Kim

Jeongsik Kim, Professor of Department of Interdisciplinary Graduate Program in Advanced Convergence Technology and Science, Jeju National University

Department of Interdisciplinary Graduate Program in Advanced Convergence Technology and Science
GRADUATE SCHOOL
JEJU NATIONAL UNIVERSITY

CONTENTS

List of Abbreviations

ACD6	:	ACCELERATED CELL DEATH 6
DAE	:	Days after emergence
DAT	:	Days after treatment
EMMA	:	Efficient mixed model association
ETR	:	Electron transport rate
FC	:	Fluorescence camera
FDR	:	False discovery rate
GVS1	:	GENETIC VARIANTS IN LEAF SENESCENCE 1
GWA	:	Genome-wide association
HAP	:	Haplotype
IR	:	Infrared
MAF	:	Minor allele frequency
NMR19-4	:	Naturally occurring DNA methylation variation region19-4
ORE1	:	ORESARA1
PC	:	Principal components
PCR	:	Polymerase chain reaction
PHI	:	Phenome high-throughput investigator
QTL	:	Quantitative trait loci
RIL	:	Recombinant inbred line
RGB	:	Red-Green-Blue
SA	:	Salicylic acid
SAG12	:	Senescence associated gene 12

SAG29	:	Senescence associated gene 29
SAGs	:	Senescence associated genes
SNP	:	Single-nucleotide polymorphism
SWIR	:	Shortwave infrared
TF	:	Transcription factor
VNIR	:	Visible and near-infrared

List of Figures

List of Tables

I. GENERAL INTRODUCTION

The leaves constitute one of the most important organs in plants. Leaves are the main sites for photosynthesis, the central life strategy of plants. The leaf developmental process is composed of many distinct stages, ranging from initiation, expansion, maturation to senescence and death (**Figure 1**). During the early stages, leaves function as autotropic organs to gather energy and resources for plant growth. Various biological processes involved in the early stages of leaf development include cell structure building, amino acid anabolism or carbon/nitrogen assimilation (Avila-Ospina et al., 2014). When leaves reach the maturation stage, the onset of leaf senescence begins. Under optimal growth conditions, leaf senescence is regulated in an age-dependent manner (Schippers et al., 2007). Different from the senescence in animals and unicellular organisms often associated with death, leaf senescence in plants requires highly integrative processes involving cell death, nutrient recycling, and storage (Koyama, 2018).

During senescence, leaf cells undergo systematic changes in their structures, their metabolism, and their sink-source relationships in a programmed manner (Thomas, 2013). Chloroplasts, which contain the majority of leaf protein, are the first organelles to be broken down, while mitochondria and the nucleus remain intact until the later stages. The structural dismantlement in cellular organelles facilitates plants in recycling a major portion of the leaf lipids and proteins for a rich source of nitrogen (Girondé et al., 2015). Metabolically, autotrophic carbon assimilation of the leaf is superseded by the catabolism of cellular organelles and macromolecules to provide

energy support for essential cellular processes during senescence. In addition, this shift in metabolic activities is important for efficiently converting cellular resources into macro- and micronutrients that will be relocated to support developing seeds or other growing organs (**Figure 1**). Therefore, senescence-mediated nutrient relocation is essential for optimal nutrient utilization and plant survival. In this regard, leaf senescence can also be considered as an evolutionarily acquired process that critically contributes to the overall fitness of the whole plant by increasing their availability for optimal offspring production and better survivability in their given temporal and spatial niches.

Over the past three decades, numerous studies employing both forward and reverse genetic approaches have revealed that leaf senescence is actively and genetically regulated by a complex, multi-layered regulatory network. Leaf senescence programs can be initiated or activated by internal age, but also they are modulated by a wide range of internal and external signals (Lim et al., 2007). The major endogenous factors that affect leaf senescence include various phytohormones and reproductive development (**Figure 1**). Multiple environmental factors, including abiotic stresses such as drought, salinity, temperature, nutrient deficiency, as well as biotic stresses such as animal/insect attacks or pathogen infection, are also critical in shaping the onset or progression of senescence (**Figure 1**). Molecular pathways that recognize these senescence-inducing factors do not work independently; instead, they are interconnected to form a complex regulatory network for senescence (Guo and Gan, 2012). Senescence, therefore, reflects the life history of the leaf experiencing senescence-associated physiology in the context of interaction between internal and

external factors. Senescence variations among natural populations may underlie the environmental and endogenous factors that influence senescence biology.

One of the key mechanisms that modulate biochemical and physiological changes during senescence progress is the modification of diverse senescence associated gene (SAG) expression. Many SAGs have been identified to be involved in senescence process, such as *SEN4* or *SAG12*, which encode xyloglucan endotransglucosylase/ hydrolase 24 and cysteine protease, respectively. These two genes function in macromolecule degradation, and their expression are upregulated during senescence (Woo et al., 2001; Lim et al., 2003). Another example is the decline in expression of various photosynthetic-related genes such as chlorophyll a/b binding protein gene and rubisco small subunit gene along the course of senescence progression (Woo et al., 2001). The modification of SAGs is regulated coordinately by the dynamic activation/inactivation of various positive and negative senescence regulatory elements. These elements belong to diverse families with distinct functions, including receptors, kinases/phosphatases, transcription factors (TFs), and epigenetic regulators. Among these, TFs play the essential roles for regulating the temperal expression of SAGs during leaf aging. Several important TF families that involve in senescence process include NACs (NAM/ATAF/CUC), WRKYs or MYBs. Time-evolving NAC networks undergo a temporal transition of regulatory interaction among NACs from the presenescent to the senescent stage and guide the timely induction of senescence processes, such as SA and ROS responses (Kim et al., 2018).

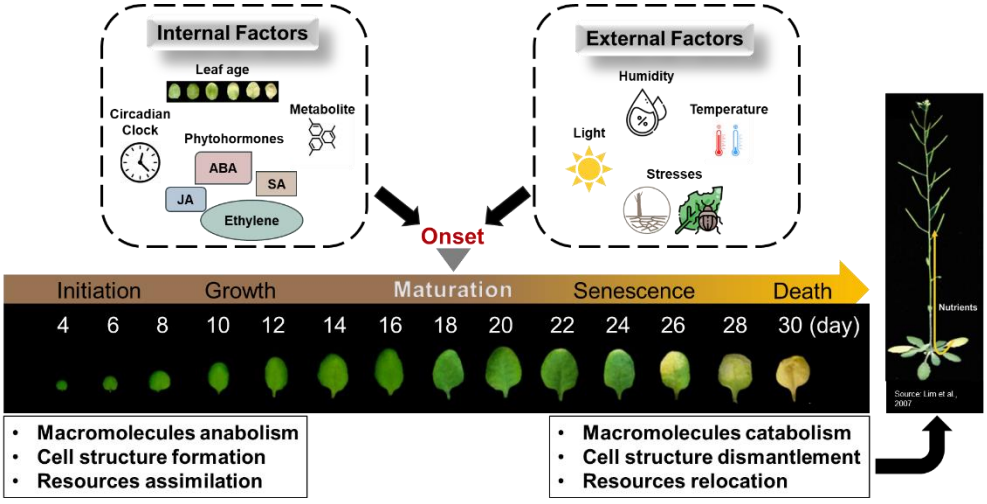

Figure 1. Leaf development and senescence process. During the early stages, leaves function as autotropic organs for nutrients and resources assimilation. When senescence occurs, biochemical activities of leaves are shifted from anabolism to catabolism for relocation of nutrients and resources to other newly developing organs or seeds. The onset and progression of leaf senescence are regulated by various internal and external factors. Figure is modified from Avila-Ospina et al., (2014) and Woo et al., (2019).

II. MAIN RESEARCH

1. SUMMARY

Leaf senescence is an evolutionarily conserved process that is essential for plants' fitness, as it adjusts the temporal balance of energy production between photosynthesis and catabolism. The onset and progression of senescence are determined by the interaction between genetic and environmental factors, making senescence one of the adaptation processes in plants around their natural habitats. In this study, I aimed to investigate the genetic basis of age-induced leaf senescence in Arabidopsis natural populations. By employing the phenome high-throughput investigator, I have successfully revealed comprehensive senescence responses among 234 Arabidopsis accessions. Additionally, I identified environmental and physiological factors that are highly associated with senescence phenotypes. Genome-wide association mapping discovered the *ACCELERATED CELL DEATH 6* (*ACD6*) locus as a potential candidate for regulating the variation of senescence responses among natural accessions. Knocking out *ACD6* in natural accessions with early and delayed senescence phenotypes resulted in different extents of delaying age-induced senescence, implying that the regulatory activities of *ACD6* in leaf senescence are accession-dependent. Furthermore, my obtained data suggest that *ACD6* is involved in the regulation of leaf senescence via the salicylic acid signaling pathway. Taken together, this study has provided molecular insights into the genetic regulation of leaf senescence in Arabidopsis natural populations, with the discovery of the key regulator

ACD6, which may be a potential candidate for genetic modification to improve plant adaptation and survival.

2. BACKGROUND

Leaf senescence is a complex yet highly regulated developmental process involving a coordinated sequence of multiple molecular events. The timing and progression of leaf senescence is crititial for plant fitness and survilability (Uauy et al. 2006). Plants requires an efficient senescence process to helps optimize their energy usage and maximize their fitness, and premature senescence induced by adverse environmental conditions significantly affect plant yield and productivity (Hortensteiner and Feller 2002). Senescence, therefore, has evolved as a life history strategy with substantial biological importance. The ultimate goal of leaf senescence research is to understand the composition, organization, and function of complex gene-regulatory networks that govern leaf senescence.

The model plant Arabidopsis originally inhabited Eurasia and Africa. However, due to its ability to thrive in poor and challenging environments, it has been introduced and naturalized rapidly around the world. Arabidopsis inhabits various geographical locations with different environmental conditions. The natural populations of Arabidopsis have an evolutionary history of drastic climatic and environmental changes. As an important life history trait that helps plants optimize their viability for next generation or season, leaf senescence may implicate environmental and evolutionary factors that influence plant biology. In this regard, Arabidopsis accessions exhibit a wide range of variations in senescence physiology, which has been shaped by environmental adaptation and influenced by genetic context (**Figure 2**).

Consequently, mutations in certain senescence regulatory genes, such as *RPK1* and *ORE1*, exhibited different levels of senescence in different genetic accessions of Col and Ler (Unpublished). Therefore, senescence studies throughout natural accessions can unravel the evolutionary and adaptive roles of senescence processes and provide insights into fundamental questions concerning the factors that shape senescence biology.

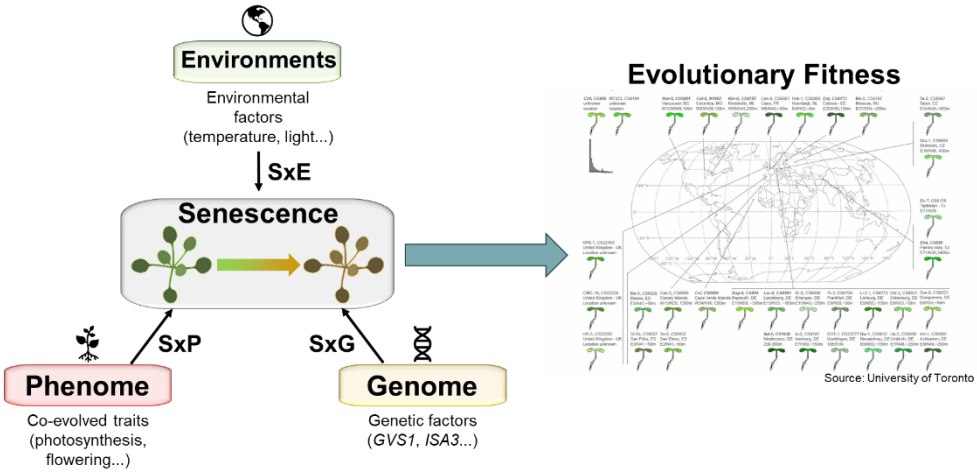

Figure 2. Leaf senescence and evolutionary fitness in natural populations. Arabidopsis habitats expand in a wide range of geographical and environmental conditions. Leaf senescence is shaped by the interaction between the genome, phenome and environment factors. As a life history trait for maximizing plant fitness, senescence phenotypes of reflect the adaptative process of Arabidopsis accessions to the natural habitats over the course of evolution. Figure is modified from Kim et al., (2018). Geographical distribution of Arabidopsis accessions was obtained from University of Toronto (http://www.bar.utoronto.ca/).

In this regard, researchers have made efforts to collect Arabidopsis accessions with ecological and climatic information from the wild, and their populations have been widely utilized. Several studies have been conducted to understand the implications of senescence programs in a group of Arabidopsis populations. The early attempts successfully elucidated the relationships between leaf senescence and other life history traits such as photosynthetic potential, reproductive efficiency, and post-

bolting longevity (Levey and Wingler 2005; Luquez et al., 2006). Quantitative traits loci (QTL) analysis using two parental lines was also employed to investigate the genetic basis of natural variation in Arabidopsis senescence programs (Luquez et al., 2006; Wingler et al., 2009). Bay-0 x Shahara recombinant inbred line (RIL) population suggested that *FRI* and *FLC* loci mediate flowering and glucose-induced senescence (Wingler et al., 2009). Recently, the natural alleles *ACCELERATED CELL DEATH 6* (*ACD6*) were reported to be responsible for senescence variation between Col-0 and Ct-1 using the QTL approach (Jasinski et al., 2021). The completion of several genome-wide sequencing projects in a large set of Arabidopsis natural populations such as the Regional Mapping Panel (Horton et al., 2012) or the 1001 Genome Consortium (2016) has further facilitated studies on the association between genetic factors and senescence responses. Genome-wide association (GWA) analyses have successfully identified several genetic loci that account for the differential senescence phenotypes in natural accessions, such as the natural alleles *GENETIC VARIANTS IN LEAF SENESCENCE1* (*GVS1*) (Lyu et al., 2019) or the epialleles *naturally occurring DNA methylation variation region19-4* (*NMR19-4*) (He et al., 2018).

In this study, I aimed to explore the genetic basis of natural diversity in age-induced leaf senescence phenotypes. I conducted phenome-based analyses using a high-throughput phenome (PHI) to investigate comprehensive senescence responses in the leaves of 259 Arabidopsis natural accessions. My findings revealed several environmental factors and physiological responses that are linked to age-induced senescence. Furthermore, a genome-wide association analysis with senescence-associated principle component factors and further phenotypic analysis of loss-of-

function mutants in potential candidates revealed that *ACD6* is involved in the regulation of age-induced leaf senescence, but not dark-induced leaf senescence. I also confirmed that *ACD6* has accession-dependent activities in SA-mediated senescence. This study suggests that the genetic diversity of *ACD6* underlies natural diversity in SA- and age-induced leaf senescence and provides genetic evidence that the regulation of leaf senescence contributes to an increase in plant fitness among Arabidopsis natural accessions.

Note: The term “ecotypes” that has been widely used previously for Arabidopsis natural accessions implies the unique ecology and adaptation of that line to a specific environment. The neutral term “accessions”, which is used as an identifier in a collection has been assigned, is more applicable in this study.

3. MATERIALS AND METHODS

3.1. Plant Materials and Growth Condition

A collection of *Arabidopsis thaliana* accessions from a previous study (Lyu et al., 2019) was used to investigate variation in senescence responses. *acd6-1* (CS72446) *acd6-2* (SALK_045869), and *acd6-11* (SALK_059132) were obtained from the Arabidopsis Biological Resource Center. *acd6-2* plants have been described previously (Todesco et al., 2010). Seeds of studied genotypes were stratified in the dark at 4 °C for 2 or 3 days prior to sowing. Plants were grown on soil in a growth room (Korea instrument, Korea) under a long day photoperiod (16-h-light/ 8-h-dark photocycle, 120 to 150 μmol m^{-2} s^{-1}) at 22 °C until reaching the appropriate growth stage for further analyses unless otherwise noted.

3.2. Phenomic Senescence Analysis

Phenomic senescence analysis was analyzed using the phenome high-throughput investigator (Photon Systems Instruments, Czech Republic) which was conducted with a user-designed protocol as previously described (Lyu et al., 2017) except for the absence of shortwave infrared (SWIR) and 3D imaging. 259 Arabidopsis natural accessions, mostly derived from the RegMap panel (Horton et al., 2012; Lyu et al., 2019) were used in this investigation. For age-induced leaf senescence, the 3rd and 4th leaves of plants at 34 days after emergence (DAE) were carefully cut from each plant with sharp scissors and arranged in an acryl plate with a 12 x 9 grid (9 leaves per accession). A total of 412 phenomic traits (99, 25, 4, and 84 traits for fluorescence camera (FC), Red-Green-Blue (RGB), Infrared (IR), visible and near-infrared (VNIR) imaging analysis, respectively) were obtained. For dark-induced leaf senescence 3rd and 4th leaves of plants at 12 DAE were cut and incubated in 3 mM MES buffer (pH 5.7) for the indicated days after dark treatment (DAT). Principal component (PC) analysis was performed using the Pearson's correlation matrix UNSCRAMBLERX 10.3 (CAMO, Oslo, Norway). The obtained PC values were used for further tests, including correlation and GWA analyses.

3.3. Association Analyses

The geographical distribution, climate data, and phenological data for each accession were obtained from a previous study (Lyu et al., 2019). Pearson correlations were used to assess the relationships between data series and statistical significance was established by comparing the correlation value of the original data with that of 10,000 permutated data sets. GWA analysis was conducted on the PC values with

AtPolyDB (minor allele frequency (MAF) > 0.1; Horton et al., 2012) using easyGWAS (Grimm et al., 2017) through the efficient mixed model association (EMMA) algorithm. A significance threshold of $\alpha = 0.05$ was applied after multiple testing corrections using false discovery rate (FDR). Manhattan plot was generated using SNPEVG (Wang et al., 2012). Linkage disequilibrium was generated with easyGWAS.

3.4. Plasmid Construction and Transgenic Plants Generation

The CRISPR/Cas9 system (Xing et al., 2014) was employed to generate a loss-of-function mutant of *ACD6* in Arabidopsis natural accessions indicated. Two synthetic oligos for the generation of sgRNA that targets *ACD6* were annealed and ligated into the *Bsa*I-linearized pBSE401 vector (**Table 1**). The obtained construct was then transformed into plants using *Agrobacterium*-mediated (AGL1 strain) floral dip method (Clough & Bent, 1998). T_1 transgenic plants were selected based on their antibiotic resistance. The genomic DNA of resistant plants were extracted for PCR amplification of fragments surrounding the target regions of *ACD6* using gene-specific primers (**Table 1**). Positive candidates were identified by their resistance to digestion with *Hpy166*II in the amplified fragment. These candidates were further tested in segregated, non-transgenic T_2 and confirmed by sequencing. Homozygous lines with aberrant *ACD6* genes were then used for subsequent analyses. The gene-specific primer sets used for plasmid construction and plant genotyping are listed in **Table 1**.

3.5. Leaf Senescence Assays

All senescence experiments were conducted using the 3rd and 4th rosette leaves. Leaves at the indicated DAE were cut with sharp scissors at 4 to 5 h after the lights

were turned on for assay age-induced leaf senescence. For dark-induced senescence, leaves at 12 DAE were also harvested at 4 to 5 h after the lights turned on and floated abaxial side up in 3 mM MES buffer (pH 5.7). Samples were completely covered with aluminum foil for the indicated DAT. For salicylic acid (SA)-induced senescence, detached leaves with 12 DAE were incubated in 3 mM MES buffer (pH 5.7) supplied with either 1.2 mM or 2.4 mM of SA, with the abaxial side down and covered with transparent wrap. 8 to 12 leaves per genotype or accession were used for the senescence assay. At DAEs or DATs indicated, leaves were used for measuring chlorophyll contents and photochemical efficiency using atLEAF^{+} Chl meter (FT Green LLC, USA) and FluorCam FC 800-C (Photon Systems Instruments, Czech Republic), respectively. Two-tailed Student's *t*-test was used to identified significant differences between *acd6* mutants and their respective backgrounds at the same leaf age/treatment conditions. To compare the effect of knocking out *ACD6* in different accesions, two-way ANOVA followed by contrast analysis was employed.

3.6. Gene Expression Analysis

Leaves of indicated DAEs or DATs were harvested for quantitative reverse transcription-PCR (qRT-PCR) Total RNA extraction (WelPrep^{TM} – WelGENE, Korea) and cDNA synthesis (ImProm-II™ Reverse Transcription – Promega, Korea) were conducted according to the manufacturer's instructions. Gene-specific primers for quantifying transcript levels were provided in **Table 1**. qRT-PCR was carried out using TOPreal^{TM} qPCR SYBR Green PreMIX (Enzynomics, Korea) and Bio-Rad CFX96 real-time PCR detection system (Bio-Rad) with the following thermal profile: 94 °C for 10 min, followed by 40 cycles of 94 °C for 10 s, 60 °C for 15 s, and 72 °C

for 30 s. The $2^{-\Delta\Delta Ct}$ method was employed to analyze the expression level of the target genes with *UBQ10* as reference. The relative values of expression were determined against the maximum value of Col-0. The experiments were repeated at least twice. Statistical analysis was performed using two-tailed Student's *t*-test to identify the significant differences between genotypes or treatments.

Table 1. List of oligos

Name	Sequence (5' to 3')
Oligos for cloning	
ACD6-guideCAS-F	attgGCTACCTGTCTGGTGAACG
ACD6-guideCAS-R	aaacCGTTCACCAGACAGGTAGC
Primers for genotyping	
ACD6-Cas-F	TCATGGCGGTCATACCAAAG
ACD6-Cas-R	TCTACGGCTTCGTACAAGGA
Primers for qRT-PCR	
ORE1-qPCR-F	AATGAAGCTGTTGCTTGACG
ORE1-qPCR-R	AGAAATTCCAAACGCAATCC
SAG12-qPCR-F	AAAGGAGCTGTGACCCCTATCAA
SAG12-qPCR-R	CCAACAACATCCGCAGCTG
SAG29-qPCR-F	GCCACCAGGGAGAAAAGG
SAG29-qPCR-F	CCACGAAATGTGTTACCATTAGAA
UBQ10-qPCR-R	GGCCTTGTATAATCCCTGATGAAT

UBQ10-qPCR-R	AGAAAGAGATAACAGGAACGGAAAC

4. RESULTS

4.1. Investigation of age-induced senescence responses among natural accessions

Leaf senescence in natural conditions is mainly determined by acquired genetic programs that have been shaped by environmental and physiological responses in plants along aging. Therefore, age-induced senescence reflects the adaptive role of senescence in a given environment. My previous research showed that Arabidopsis natural accessions exhibit a wide range of dark-induced leaf senescence phenotypes which are under moderate to strong genetic control (Lyu et al., 2019). However, dark-induced leaf senescence fails to take into account many aspects of senescence programs and cannot fully reflect natural senescence responses. To gain a natural understanding of leaf senescence responses in Arabidopsis natural accessions, I quantitatively evaluated 412 phenomic traits from 34-day-old detached leaves of plants among 259 natural accessions using a high-throughput investigator consisting of various imaging units such as RGB, fluorescence, and VNIR imaging (**Figure 3**; Lyu et al., 2017). I also conducted a correlation test between age- and dark-induced leaf senescence among my examined accessions (**Figure 4**). The result showed that there was only a weak correlation between age- and dark-induced senescence responses, further confirming the potential differences in regulatory mechanisms between these two pathways.

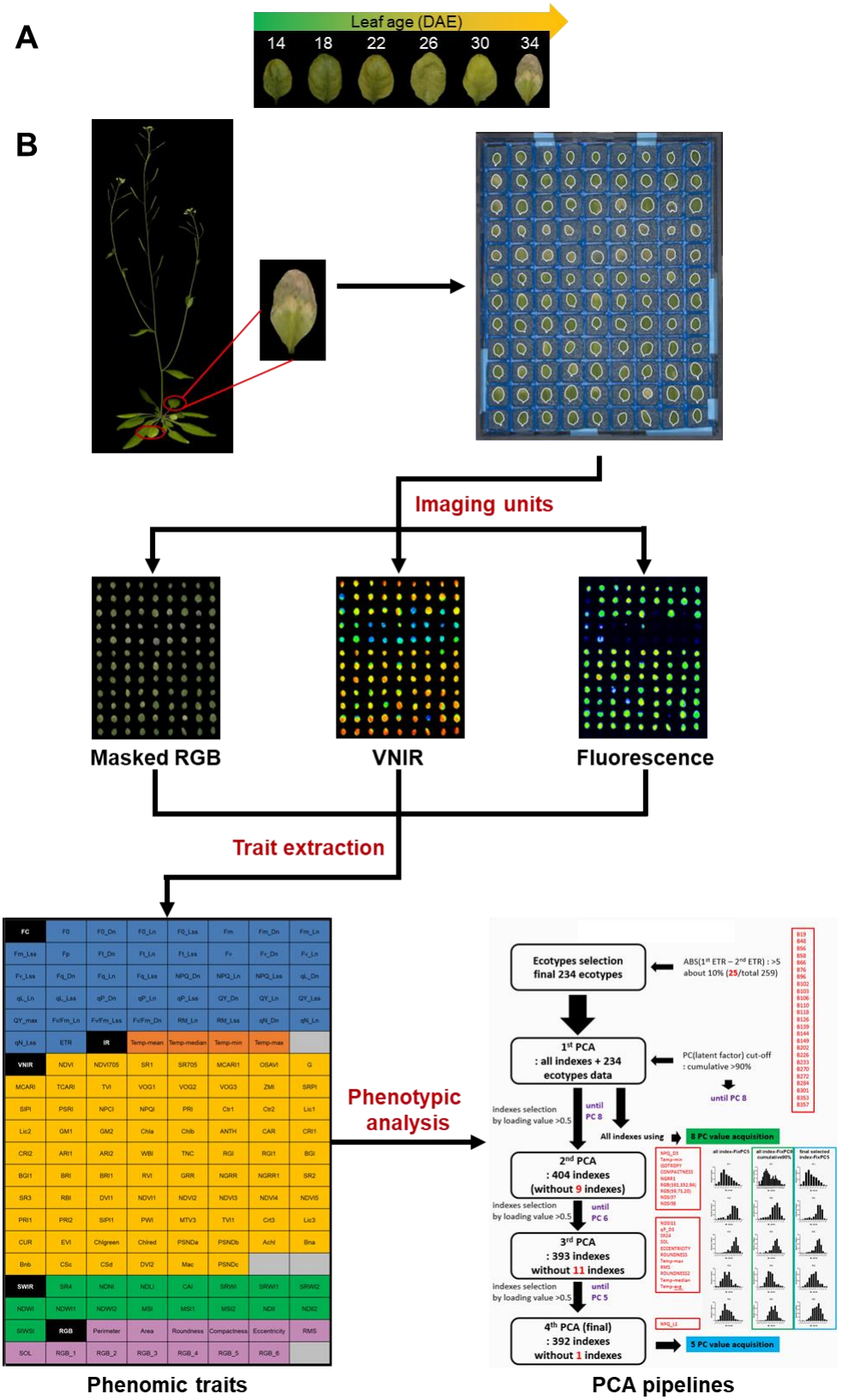

Figure 3. Scheme and workflow of phenotypic analysis of age-induced senescence using high-throughput investigator (PHI). (**A**) Phenotypes of 3rd and 4th leaves of Arabidopsis reference accessions Col-0 from maturation to senescence. (**B**) Workflow for phenotypic analysis of age-induced leaf senescence in Arabidopsis natural accessions. 3rd and 4th leaves (34 DAE) of accessions were harvested (9 leaves/accession). Phenomic traits were extracted from various imaging data. The experiment was repeated twice and senescence phenotypes were analyzed using the mean values of two trials. Only representative phenomic traits for each imaging unit were presented in this figure.

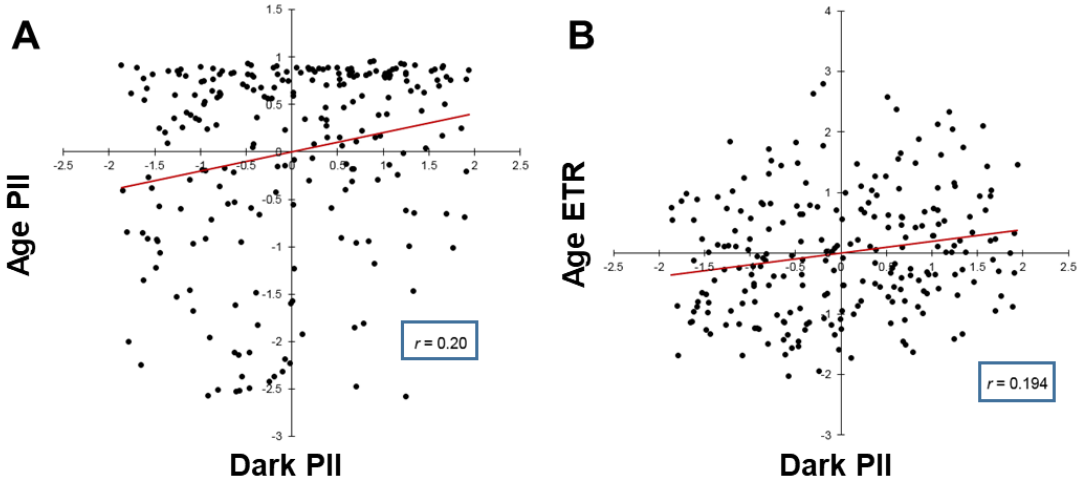

Figure 4. Pearson correlation test between age- and dark-induced senescence phenotypes among 234 Arabidopsis natural accessions. Correlation of photochemical efficiency of photosystem II during dark-induced leaf senescence (Dark PII) with (**A**) photochemical efficiency of photosystem II during age-induced leaf senescence (Age PII) and (**B**) electron transport rates during age-induced leaf senescence (Age ETR).

4.2. Analysis of leaf physiological indexes during age-induced leaf senescence

I applied principal component analysis to reduce the dimensionality of the data set and to identify features that explain senescence processes. The top three PCs were found to separate the phenotypes of accessions and account for most of the variability (**Figure 5**). The variations explained by PC1 to 3 were 50.1, 22.1, and 11%, respectively (**Figure 5A**). The Pearson correlation coefficients among PC values showed the highest correlation between PC1 and PC2 (0.75) and between PC2 and

PC3 (0.64) (**Figure 5B**). Therefore, PC1, PC2 and PC3 were considered major PCs that are related to age-induced senescence responses. PC values for each accessions are available online (https://shorturl.at/xFIMT). Two independent trials were conducted and the mean values of the two trials were used for subsequent analyses. 25 accessions were excluded in principle component analysis due to high variation in phenotypes between the two trials (the difference in their electron transport rate (ETR) values between the two trials was above 5). I also conducted hierarchical clustering analyses of traits among PC values to identify a group of traits linked to each PC (**Figure 5C**). For example, PC1 showed a positive and high correlation with ETR and GM1 indexes and a negative and high correlation with DSSI1 and Yellowing indexes. On the other hand, PC2 was highly associated with the photochemical efficiency in photosystem II (F_v/F_m), PRI1, PSRI, and qP_LSS indexes.

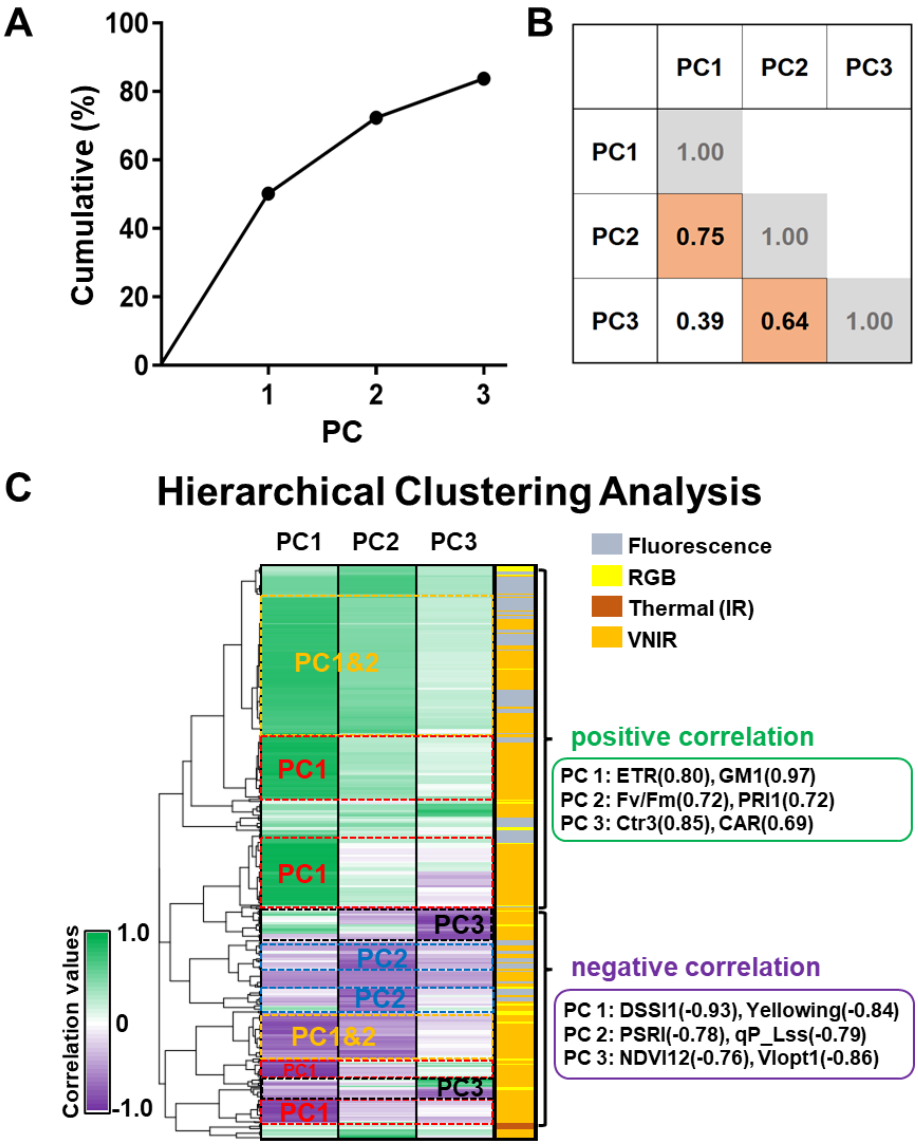

Figure 5. Principal component analysis (PCA) for age-induced leaf senescence responses from 234 natural accessions. (**A**) The explanatory accumulation of PC1-3. (**B**) Pairwise correlation between the three major PCs. (**C**) Hierarchical clustering analysis with numeric traits that are associated with each PC component. ETR: electron transport chain; GM1: Gitelson and Merzlyak index 1; F_v/F_m: variable fluorescence/maximum fluorescence; PRI1: photochemical reflectance index 1; Ctr3: Carter index 3; CAR: carotenoid reflectance index; DSSI1: damage sensitive spectral index 1; Yellowing: yellowing ratio; PSRI: plant senescence reflectance index; qP_Lss: photochemical quenching of variable chlorophyll fluorescence based on a lake model for the photosynthetic unit_light steady-state; NDVI12: normalized difference vegetation index 12; Vlopt1: optimized vegetation index 1. Further information regarding phenomic traits in this study are available in Lyu et al. (2017).

4.3. Correlation between PCs and biological or environmental conditions of their habitats among natural accessions

Arabidopsis habitats spread in a wide range of areas under various geographic and climatic conditions. As an important process to improve plant fitness, the divergent of leaf senescence programs in Arabidopsis natural accessions could be the result of evolution to adapt to different environments. To provide insight into the adaptive roles of senescence, I identified the association between major PCs related to age-induced senescence responses and 90 environmental variables from 234 accessions (**Figure 6A**). Among the three examined PCs, PC2 displayed weak but significant correlations with most of the factors related to geography, humidity, seasonality, and temperature. Particularly, PC2 was positively associated with monthly temperature and humidity and negatively associated with geographical locations. It is noteworthy that although only correlated with certain factors, PC1 and PC3 were complementary with PC2 in terms of association with environmental variables. This implies that external conditions are substantially attributed to senescence responses and the variation of leaf senescence in Arabidopsis natural accessions is the result of the adaptative process. I also conducted correlation tests between plant dark-induced leaf senescence and the examined environmental variables (**Figure 6A**). Interestingly, the results indicated different patterns between dark-induced and age-induced in association with environmental factors. Except for humidity, dark-induced leaf senescence displayed nearly no correlation with other external factors, including geographic, seasonal, and temperature (**Figure 6A**). This finding suggested that the effects of environmental

conditions on plant dark-induced senescence responses are weaker compared to age-induced senescence among Arabidopsis natural accessions.

Senescence processes likely coevolve with developmental and physiological responses via natural selection (Roach, 1994). Thus, I performed a meta-analysis to assess the relationship between senescence responses and other physiological traits (Atwell et al., 2010). I analyzed 120 phenotypes related to defense, development, flowering, ion, and senescence in Arabidopsis natural accessions (**Figure 6B**). Similar to environmental factors, PC2 displayed associations with more physiological traits compared to PC1 and PC3. Defense-related traits such as disease and bacterial resistance showed moderate negative correlations with senescence responses. On the other hand, there was a positive correlation between flowering and leaf senescence. Furthermore, I observed a relationship between senescence responses and leaf cellular ion contents. Senescence was positively correlated with lithium and calcium concentration and was negatively correlated with phosphorus and copper concentration. In contrast with age-induced leaf senescence, dark-induced leaf senescence displayed nearly no correlation with my examined phenotypes (**Figure 6B**). These results further confirm the differences between age-induced and dark-induced leaf senescence in Arabidopsis natural populations. My findings indicate that the natural variation of senescence responses in Arabidopsis accessions might be attributed to their interaction with different environmental and physiological factors.

A PxE Enrichment

		PC1		PC2		PC3		Dark PII	
Categories	Environments factor	Correlation	*P* value	Correlation	*P* value	Correlation	*P* value	Correlation	*P* value
Geo	Latitude	0.05	0.2233	-0.15	0.0045	-0.09	0.0767	0.10	0.0557
	Longitude	-0.05	0.2356	-0.13	0.0246	-0.05	0.2281	-0.16	0.0067
	Latitude (Euro)	0.01	0.4391	-0.14	0.0217	-0.02	0.4145	0.05	0.2499
	Longitude(Euro)	-0.03	0.3392	-0.14	0.0267	0.06	0.2040	-0.19	0.0025
Humidity	Jan_P	0.04	0.2771	0.09	0.0771	-0.01	0.4431	0.20	0.0012
	Feb_P	0.00	0.4758	0.15	0.0077	0.01	0.4707	0.15	0.0094
	Mar_P	0.00	0.4946	0.16	0.0040	0.01	0.4442	0.17	0.0053
	Apr_P	0.01	0.4413	0.15	0.0057	0.06	0.1941	0.10	0.0603
	May_P	-0.01	0.4471	0.14	0.0144	0.07	0.1292	0.06	0.1935
	Sep_P	0.01	0.4004	0.09	0.0788	0.07	0.1334	0.08	0.1097
	Oct_P	0.05	0.2312	0.15	0.0068	0.05	0.2322	0.14	0.0136
	Nov_P	0.05	0.2449	0.13	0.0195	0.03	0.3531	0.18	0.0030
	Dec_P	0.04	0.2804	0.11	0.0378	-0.02	0.3880	0.21	0.0005
	Preci_sum	0.04	0.2734	0.09	0.0741	-0.01	0.4318	0.20	0.0007
	Aridity index	0.05	0.2356	0.14	0.0126	0.00	0.4850	0.18	0.0055
	Bio12_ann_prec	0.05	0.2453	0.16	0.0102	0.07	0.1800	0.16	0.0109
	Bio13_prec_wm	0.05	0.2600	0.15	0.0140	0.06	0.1912	0.08	0.1335
	Bio14_prec_dm	0.03	0.3256	0.14	0.0270	0.08	0.1147	0.18	0.0054
	Bio15_prec_cv	-0.04	0.3084	-0.01	0.4332	0.02	0.4331	-0.16	0.0130
	Bio16_prec_wetq	0.05	0.2186	0.14	0.0179	0.04	0.2747	0.09	0.0973
	Bio17_prec_dryq	0.04	0.2996	0.15	0.0138	0.08	0.1222	0.18	0.0045
	Bio18_prec_warmq	-0.01	0.4251	0.16	0.0057	0.05	0.2492	0.15	0.0197
	Bio19_prec_coldq	0.04	0.2674	-0.06	0.1886	0.01	0.4299	0.18	0.0058
	RH_winter	0.15	0.0123	0.03	0.3359	-0.02	0.3961	0.25	0.0001
	RH_spring	0.15	0.0159	0.01	0.4291	-0.05	0.2522	0.21	0.0028
	RH_summer	0.09	0.0881	-0.06	0.2086	-0.02	0.4230	0.19	0.0034
	RH_fall	0.05	0.2346	0.14	0.0132	0.00	0.4905	0.18	0.0045
Seasonal	Aridity_fao	0.10	0.0882	-0.07	0.1621	0.02	0.4070	0.01	0.4238
	PAR_spring	0.12	0.0451	0.10	0.0709	0.01	0.4585	0.13	0.0298
	Length of the growing season	0.01	0.4397	-0.16	0.0178	-0.06	0.2066	-0.07	0.1808
	Number of consecutive cold days	0.15	0.0111	0.03	0.3582	-0.02	0.3986	0.25	0.0001
	Relative humidity_spring	-0.02	0.4087	-0.15	0.0171	-0.01	0.4403	0.03	0.3131
	Daylength spring	0.03	0.3180	0.07	0.1492	-0.01	0.4682	-0.08	0.1398
	Bio2_diur_rng	0.04	0.3113	0.22	0.0017	0.01	0.4474	0.13	0.0288
	Bio3_isotherm	0.00	0.4920	-0.16	0.0099	-0.01	0.4372	-0.18	0.0056
	Bio4_temp_season	0.10	0.0882	-0.07	0.1621	0.02	0.4070	0.01	0.4238
	PAR_spring	-0.12	0.0412	0.00	0.4943	0.11	0.0483	-0.10	0.0868
	PAR_summer	-0.04	0.3206	0.06	0.1880	0.03	0.3342	0.00	0.4845
	Slope	-0.13	0.0386	0.00	0.4098	0.05	0.3192	-0.06	0.3157
	FAO_agriculture_gt75percent	0.03	0.3346	0.05	0.2235	0.01	0.4634	-0.04	0.2956
	GGD_crop_mixed	-0.03	0.3991	-0.12	0.1023	-0.07	0.2128	-0.14	0.0618
	FAO_urban_gt50perAS	0.01	0.4345	-0.05	0.2108	-0.11	0.0584	0.03	0.3083
	GGD_developed	0.02	0.3549	-0.07	0.1500	-0.09	0.1146	0.06	0.2123
	GGD_dev_ptlydev	0.12	0.0441	0.10	0.0682	0.01	0.4512	0.13	0.0307
	LGSP_recode	0.01	0.4555	-0.16	0.0196	-0.06	0.2032	-0.07	0.1828
	Frosty_day	0.02	0.3776	0.15	0.0183	0.01	0.4546	-0.03	0.3172
	DLL_winter	-0.02	0.4025	-0.15	0.0194	-0.01	0.4419	0.03	0.3176
	DLL_spring	-0.02	0.3894	-0.15	0.0160	-0.01	0.4497	0.03	0.3235
	DLL_summer	0.02	0.3981	0.15	0.0179	0.01	0.4528	-0.03	0.3270
Temperature	DLL_fall	-0.01	0.4228	0.12	0.0309	0.05	0.2122	0.00	0.4936
	Jan_T	-0.01	0.4468	0.13	0.0273	0.04	0.2429	-0.01	0.4646
	Feb_T	0.00	0.4997	0.15	0.0122	0.04	0.2762	-0.01	0.4119
	Mar_T	0.00	0.4817	0.16	0.0061	0.02	0.3730	-0.06	0.1795
	Apr_T	0.01	0.4719	0.13	0.0218	0.00	0.4904	-0.09	0.0779
	May_T	-0.02	0.3517	0.13	0.0227	0.01	0.4303	-0.09	0.0822
	Jun_T	-0.05	0.2332	0.11	0.0379	0.03	0.3100	-0.09	0.0942
	Jul_T	-0.05	0.2468	0.13	0.0200	0.04	0.2689	-0.08	0.1135
	Aug_T	-0.04	0.2866	0.16	0.0063	0.06	0.2032	-0.05	0.2358
	Sep_T	-0.04	0.2640	0.17	0.0035	0.07	0.1384	-0.04	0.2709
	Oct_T	-0.04	0.2831	0.15	0.0073	0.07	0.1404	-0.04	0.2937
	Nov_T	-0.02	0.4032	0.12	0.0325	0.05	0.1994	-0.01	0.4219
	Dec_T	-0.02	0.3552	0.15	0.0068	0.05	0.2180	-0.04	0.2583
	Temp_avg	-0.02	0.4095	0.02	0.3763	0.01	0.4622	-0.07	0.1711
	Bio5_maxT_wm	-0.02	0.4125	0.13	0.0357	0.02	0.3990	0.13	0.0263
	Bio6_minT_cm	0.00	0.4764	-0.11	0.0661	-0.01	0.4465	-0.17	0.0049
	Bio7_temp_annrange	0.06	0.2028	-0.11	0.0653	0.02	0.3972	-0.04	0.3213
	Bio8_meanT_wet	-0.05	0.2260	0.16	0.0110	0.10	0.0747	0.10	0.0890
	Bio9_meanT_dry	-0.02	0.3706	0.02	0.4198	0.03	0.3532	-0.05	0.2463
	Bio10_meanT_warm	-0.02	0.4112	0.14	0.0244	0.03	0.3375	0.11	0.0510
	Bio11_meanT_cold	0.02	0.3680	0.12	0.0425	0.00	0.4962	0.07	0.1560
	Thermal_recode	-0.02	0.4039	0.14	0.0227	0.03	0.3293	0.12	0.0544
	Tmean_win	-0.02	0.3711	0.01	0.4334	0.03	0.3468	-0.05	0.2573
	Tmean_sum	-0.02	0.3752	0.01	0.4346	0.03	0.3433	-0.05	0.2489

B PxP Enrichment

		PC1		PC2		PC3		Dark PII	
Categories	Experiment Description	Correlation	*P* value	Correlation	*P* value	Correlation	*P* value	Correlation	*P* value
Defense	Resistance to H. parasitica_Emco5	0.10	0.2699	-0.04	0.4134	0.13	0.2061	0.30	0.0266
	Resistance to P. parasitica_Emwa1	0.06	0.3549	-0.36	0.0084	0.17	0.1487	-0.18	0.1382
	Resistance to P. parasitica_Emoy	0.11	0.2438	-0.17	0.1445	0.04	0.3965	0.03	0.4374
	Resistance to H. parasitica_Hiks1	0.15	0.1756	-0.25	0.0541	0.23	0.0786	-0.22	0.0863
	Resistance to P. parasitica_Noco2	-0.15	0.1647	-0.18	0.1222	0.07	0.3105	-0.03	0.4122
	Resistance to avrPphB	0.05	0.3706	0.25	0.0635	-0.01	0.4738	0.30	0.0279
	Resistance to avrRpm1	-0.09	0.2918	-0.37	0.0052	0.29	0.0385	0.02	0.4463
	Resistance to avrRpt2	0.03	0.4309	0.22	0.0938	0.02	0.4203	0.03	0.4204
	Resistance to avrB	-0.15	0.1764	-0.38	0.0052	0.21	0.0961	-0.02	0.4471
	Susceptible to Pseudomonas LP23.1a	-0.19	0.0548	-0.28	0.0133	0.08	0.2425	-0.15	0.0968
	Susceptible to Pseudomonas LP23.1a	0.13	0.1238	0.02	0.4342	0.01	0.4493	0.26	0.0325
	Susceptible to Pseudomonas RMX23.1a	-0.10	0.2081	-0.27	0.0148	0.24	0.0151	0.13	0.1319
	Susceptible to Pseudomonas RMX23.1a	-0.06	0.3086	-0.21	0.0392	-0.12	0.1489	0.04	0.3524
	Susceptible to Pseudomonas ME3.1b	-0.04	0.3652	0.28	0.0092	-0.17	0.0775	-0.09	0.2243
	Susceptible to Pseudomonas PNA3.3a	-0.30	0.0031	-0.24	0.0280	0.15	0.0995	-0.10	0.1960
	Susceptible to Pseudomonas RMX3.1b	-0.18	0.0659	-0.30	0.0088	0.30	0.0032	0.00	0.4931
	Susceptible to Pseudomonas RMX3.1b	0.04	0.3781	-0.20	0.0393	0.08	0.2436	0.08	0.2485
	Trichome density; control water treated	0.06	0.3434	-0.25	0.0650	0.28	0.0214	-0.03	0.4191
	Trichome density; JA treated	0.03	0.4124	-0.22	0.0894	0.08	0.3210	0.04	0.3887
	Aphid offspring	0.02	0.4309	0.16	0.1387	-0.09	0.2640	-0.23	0.0593
	Bacterial titer	0.20	0.0927	0.25	0.0526	0.04	0.3923	0.09	0.2784
Development	Seed dormancy level	0.12	0.2256	0.32	0.0159	0.09	0.3037	0.21	0.1058
	Flowering period duration in GH	0.26	0.0182	0.07	0.3015	0.01	0.4847	0.00	0.4919
	Life cycle period in GH	0.13	0.1456	0.13	0.1513	0.12	0.1609	0.11	0.1773
	Maturation period	-0.19	0.0585	-0.12	0.1607	-0.19	0.0491	-0.19	0.0653
	Reproduction period	0.12	0.1658	-0.03	0.3901	-0.16	0.0982	-0.16	0.0848
	Fresh weight	0.27	0.0426	0.22	0.0747	-0.02	0.4402	0.13	0.2014
	Dry weight	0.22	0.0705	0.31	0.0191	-0.12	0.2168	0.14	0.1904
	Silique length	-0.05	0.3845	0.24	0.0467	0.03	0.4352	-0.09	0.2913
	Days to germination at 16°C	-0.06	0.2990	-0.24	0.0284	0.08	0.2545	-0.11	0.1804
	Plant diameter at 10°C	0.10	0.1978	0.33	0.0013	-0.01	0.4564	0.16	0.0795
	Plant diameter at 22°C	0.26	0.0117	0.16	0.0895	-0.10	0.1972	0.03	0.3980
	Level of leaf serration at 10°C	0.05	0.3239	-0.03	0.4136	-0.18	0.0616	-0.05	0.3273
	Level of leaf serration at 22°C	0.06	0.3079	0.06	0.2964	-0.21	0.0371	-0.01	0.4654
	Leaf roll presence at 10°C	0.17	0.0661	0.18	0.0697	0.02	0.4196	0.11	0.1780
	Leaf roll presence at 22°C	0.18	0.0628	0.22	0.0241	-0.24	0.0249	0.01	0.4464
	Presence of rosette errectness	-0.10	0.2041	0.13	0.1395	0.25	0.0167	0.11	0.1786
	Hypocotyl length	-0.20	0.0974	0.29	0.0286	-0.23	0.0654	-0.08	0.3047
	Seedling growth rate	-0.32	0.0090	0.11	0.2152	-0.15	0.1465	0.08	0.2851
	Vegetative growth rate after VER	-0.24	0.0353	0.15	0.1343	-0.06	0.3132	-0.13	0.1764
	Decrease in GR after prolonged VER	0.02	0.4495	-0.26	0.0497	0.07	0.3253	-0.21	0.0725
	Germination in the dark	-0.03	0.4345	0.31	0.0130	-0.06	0.3423	0.30	0.0177
	Duration of dry storage for 50% seed GR	0.21	0.0665	0.27	0.0188	-0.11	0.2096	0.19	0.0863
	Non-monotonous dynamic of DR	-0.03	0.4162	-0.05	0.3648	0.25	0.0452	-0.16	0.1319
	Dry storage during 7 days	-0.27	0.0176	-0.19	0.0862	0.12	0.2053	-0.04	0.3854
	Dry storage during 28 days	-0.31	0.0092	-0.27	0.0269	0.13	0.1753	-0.11	0.2142
	Dry storage during 56 days	-0.23	0.0426	-0.28	0.0164	0.12	0.1832	-0.08	0.2809
Flowering	Days to FT under LD	-0.12	0.1607	0.03	0.4381	0.24	0.0072	0.05	0.3326
	Days to FT under SD	-0.05	0.3373	-0.04	0.3518	0.27	0.0066	-0.10	0.2188
	Days to FT under SD w/ VER	0.04	0.3627	-0.22	0.0350	0.09	0.2362	-0.19	0.0575
	FT at 10°C	0.10	0.1848	-0.04	0.3313	0.24	0.0104	0.17	0.0529
	FT at 16°C	0.01	0.4325	-0.02	0.3818	0.25	0.0023	0.08	0.2419
	FT at 22°C	-0.10	0.1797	-0.10	0.1634	0.25	0.0017	-0.03	0.4007
	Days to FT under LD w/o VER	-0.04	0.3851	0.00	0.4816	0.24	0.0191	0.14	0.1341
	Days to FT under LD w/ 2W VER	-0.09	0.2311	-0.10	0.2083	0.23	0.0139	-0.02	0.4360
	Days to FT under LD w/ 4W VER	-0.06	0.3567	-0.12	0.1886	0.23	0.0223	-0.02	0.4474
	FLC gene expression	-0.08	0.2503	0.22	0.0221	0.13	0.1412	-0.07	0.2935
	Greenhouse LN at FT w/ 8W VER	0.05	0.3261	-0.03	0.3900	0.06	0.3040	-0.10	0.2133
	Greenhouse FT w/o VER	-0.10	0.2091	-0.08	0.2453	0.27	0.0024	-0.15	0.1097
	Greenhouse LN at FT w/o VER	-0.01	0.4804	0.21	0.0328	0.13	0.1378	0.15	0.1060
	Days to FT in the field	0.06	0.3292	-0.23	0.0169	0.13	0.1331	0.01	0.4585
	Days to FT in the GH	-0.06	0.3333	0.16	0.0769	0.20	0.0277	0.07	0.2926
	Leaf number at FT at 10°C	0.05	0.3417	0.00	0.4748	0.13	0.1291	-0.07	0.2742
	Leaf number at FT at 16°C	0.11	0.1828	0.11	0.1806	0.22	0.0252	0.01	0.4573
	Leaf number at FT at 22°C	-0.10	0.2093	-0.05	0.3085	0.23	0.0085	-0.13	0.1473
Ion	Lithium concentration	0.26	0.0422	0.19	0.1065	-0.01	0.4903	0.08	0.2935
	Boron concentration	0.18	0.1162	0.11	0.2277	-0.03	0.4193	-0.15	0.1711
	Magnesium concentration	0.11	0.2225	0.22	0.0739	-0.08	0.3123	0.26	0.0382
	Phosphorus concentration	-0.35	0.0059	-0.14	0.1878	0.19	0.0987	0.13	0.1887
	Sulfur concentration	-0.12	0.2025	-0.21	0.0901	0.04	0.4075	-0.20	0.0936
	Calcium concentration	0.02	0.4463	0.26	0.0468	-0.07	0.3242	0.24	0.0618
	Iron concentration	-0.18	0.1127	-0.19	0.1068	-0.16	0.1347	-0.15	0.1599
	Copper concentration	-0.27	0.0386	-0.26	0.0442	0.03	0.4312	-0.15	0.1681
	Zinc concentration	-0.04	0.4183	-0.21	0.0828	-0.03	0.4213	-0.25	0.0491
Senescence	Selenium concentration	0.12	0.1549	0.13	0.1288	0.15	0.0941	0.15	0.1095
	Last flower senescence	-0.27	0.0346	-0.44	0.0015	0.12	0.2199	0.00	0.4908
	Presence or absence of LES	-0.10	0.2949	0.03	0.4798	0.13	0.1981	0.11	0.2332
	Presence or absence of YEL	-0.30	0.0212	-0.40	0.0046	0.17	0.1336	0.05	0.3710
	Presence or absence of LES or YEL	-0.18	0.0616	0.06	0.3390	0.26	0.0047	-0.09	0.2321
	Visual chlorosis presence at 10°C	-0.06	0.2948	-0.24	0.0227	0.05	0.3467	0.04	0.3875
	Visual chlorosis presence at 16°C	0.02	0.4368	-0.16	0.0915	0.22	0.0281	0.06	0.2951
	Visual chlorosis presence at 22°C	0.02	0.4342	0.26	0.0101	-0.05	0.3238	0.18	0.0654

Figure 6. Environmental factors and physiological responses associated with age-induced and dark-induced senescence responses. Photochemical efficiency under the dark and three major PC components were used for association tests with 90 environmental factors (**A**) and 120 physiological responses (**B**). *p*-values were estimated with permutation tests. Dark PSII: photochemical efficiency of photosystem II during dark-induced senescence; JA: jasmonic acid; GH: greenhouse; GR: germination rate; DR: dormancy release; FT: flowering time; LD: long day; SD: short day; LN: leaf number; VER: vernalization LES: lesioning; YEL: yellowing.

4.4. Identification of natural alleles association with age-induced senescence responses

Senescence responses are the result of the interaction between genetic and environmental factors. GWA analysis was employed to uncover genetic loci responsible for the divergence of natural senescence programs. I performed a genome scan for single-nucleotide polymorphisms (SNPs) associated with major PC values related to age-induced senescence in Arabidopsis natural accessions (**Figure 7**). The efficient mixed model association (EMMA) algorithm was applied for this association analysis with a significance threshold of $\alpha = 0.05$ after multiple testing corrections using false discovery rate (FDR). I identified a significant SNP with the lowest *p*-value that is associated with PC2 (**Figure 7B**). However, I failed to uncover any significant SNPs that are associated with PC1 and PC3 (**Figure 7A,C**). The identified SNP is located near one locus, *At4g14400*, which contains a gene encoding for *ACD6*. This result is consistent with a previous study, in which *ACD6* was identified as causal gene for leaf senescence variations using the QTL approach (Jasinski et al., 2021). *ACD6* is specifically expressed in leaf tissues over the entire leaf lifespan in an age-dependent manner (eFP Browser, Winter et al., 2007; Andriankaja et al., 2012; Woo et al., 2016). ACD6 protein contains ankyrin and transmembrane domains (Lu et al., 2003) that function as an important regulator in the SA signaling pathway in response to biotic

and abiotic stresses (Todesco et al., 2014, Pluharova et al., 2019). As photochemical efficiency is an important indicator for assessing plant senescence phenotypes, I also conducted a genome scan for SNPs associated with F_v/F_m values in age-induced leaf senescence.

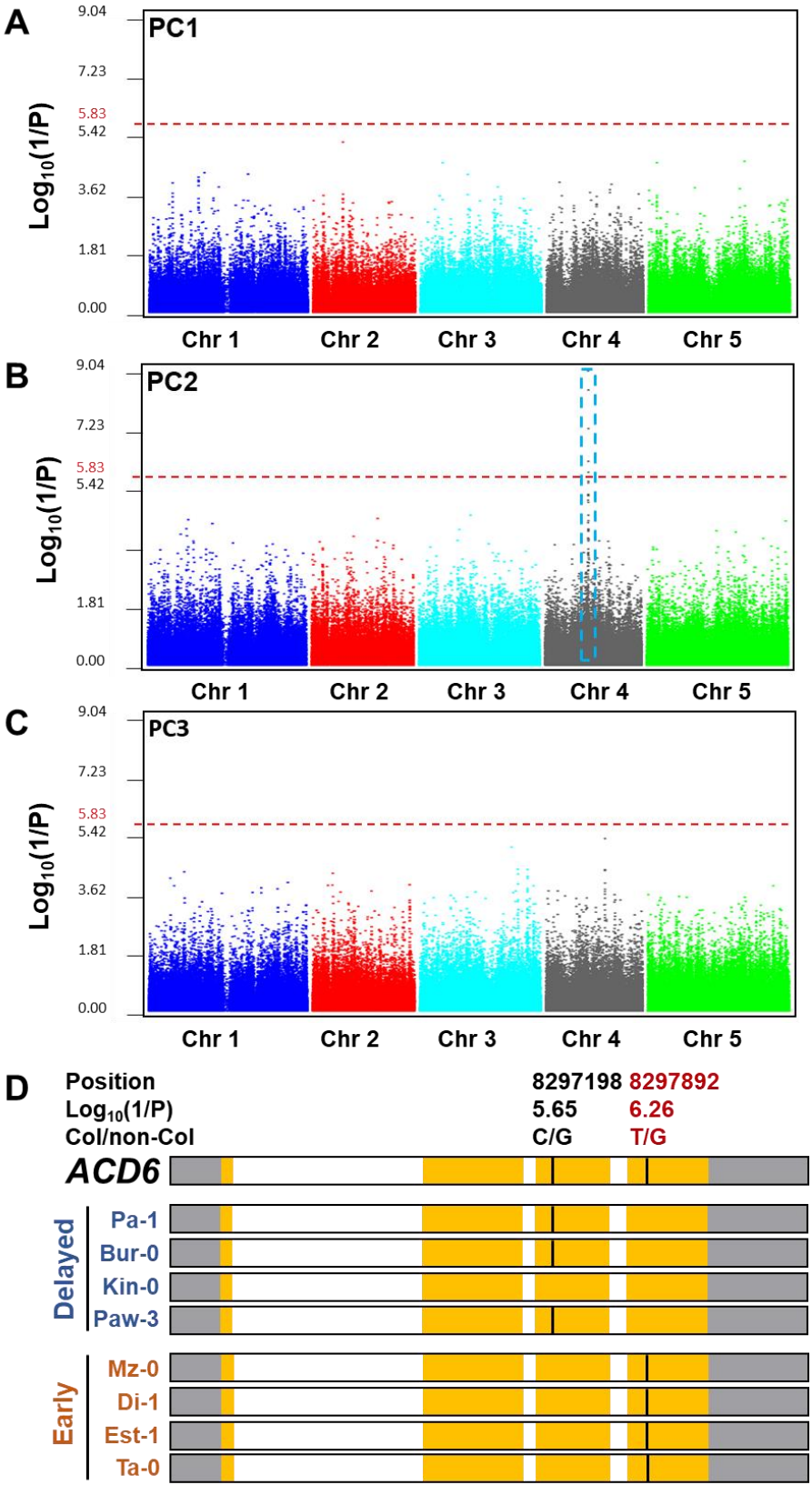

Figure 7. **Genome-wide association (GWA) mapping for PCs derived from phenomic responses by age-induced leaf senescence.** (**A-C**) Manhattan plots for age-induced leaf senescence phenotype associated with PC1, PC2, and PC3, respectively. (**D**) SNP variations of the *ACD6* gene in selected accessions with early and delayed senescence phenotypes. Gray: UTR; Yellow: exon; White: intron.

Next, I tried to uncover the association between the identified SNP with senescence phenotypes in Arabidopsis natural accessions. The identified SNP changes *ACD6* nucleotide sequence from thymine (T) in Col-0 to guanine (G) (**Figure 8**). Plants of the 'T'- and 'G'-type SNP exhibited average F_v/F_m values of 0.66 and 0.50 at 34 DAE, respectively (**Figure 8**). However, there was no clear pattern regarding geographical distribution among plants of these two SNP types (**Figure 8**).

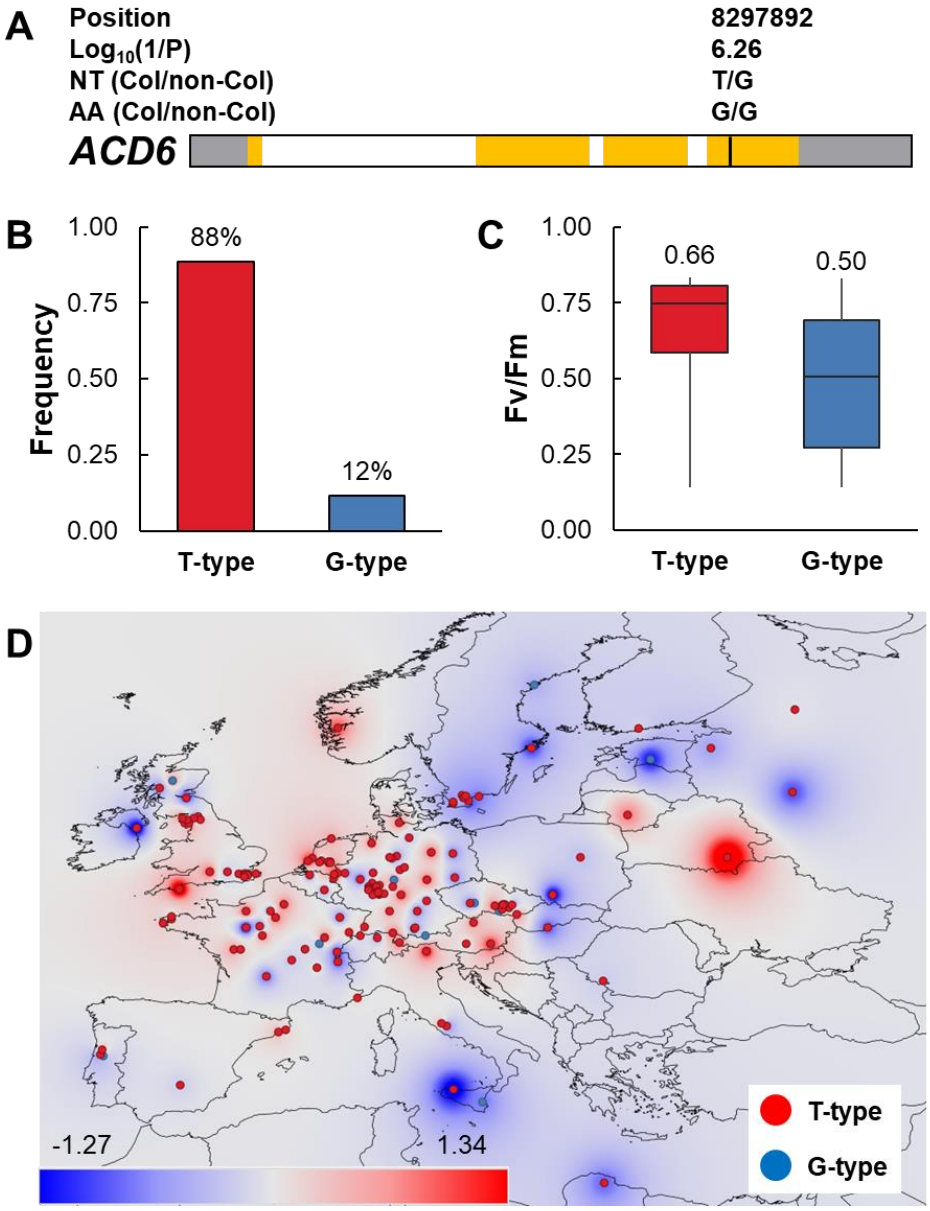

Figure 8. Geographic distribution and leaf senescence responses with respect to *ACD6* alleles. (**A**), Schematic presentation of two *ACD6* alleles. (**B**) Frequency of two *ACD6* alleles among the examined accessions. (**C**) Senescence responses of 'T-type' and 'G-type' accessions. On the box plot middle lines are the mean and whiskers above and below the box indicate the 75th and 25th percentiles. (**D**) Geographical distribution of 'T-type" and 'G-type' accessions. NT: nucleotide; AA: amino acid.

The gene cassette of *ACD6* contains two SNPs with MAF > 0.1 in the coding region (**Figure 9**). I further analyzed haplotypes (HAPs) with four different combinations of these SNPs. Among them, HAP1 and HAP4 were two major

haplotypes involving ‘T’ and ‘G’ SNPs, respectively, at 8,297,892 of Chr 4. F_v/F_m values at 34 DAE for HAP1 and HAP4 were 0.67 and 0.44, respectively (**Figure 9**). Similar to ‘T’-type and ‘G’-type SNP plants, geographical distributions of HAP1 and HAP4 were not clearly separated (**Figure 9**).

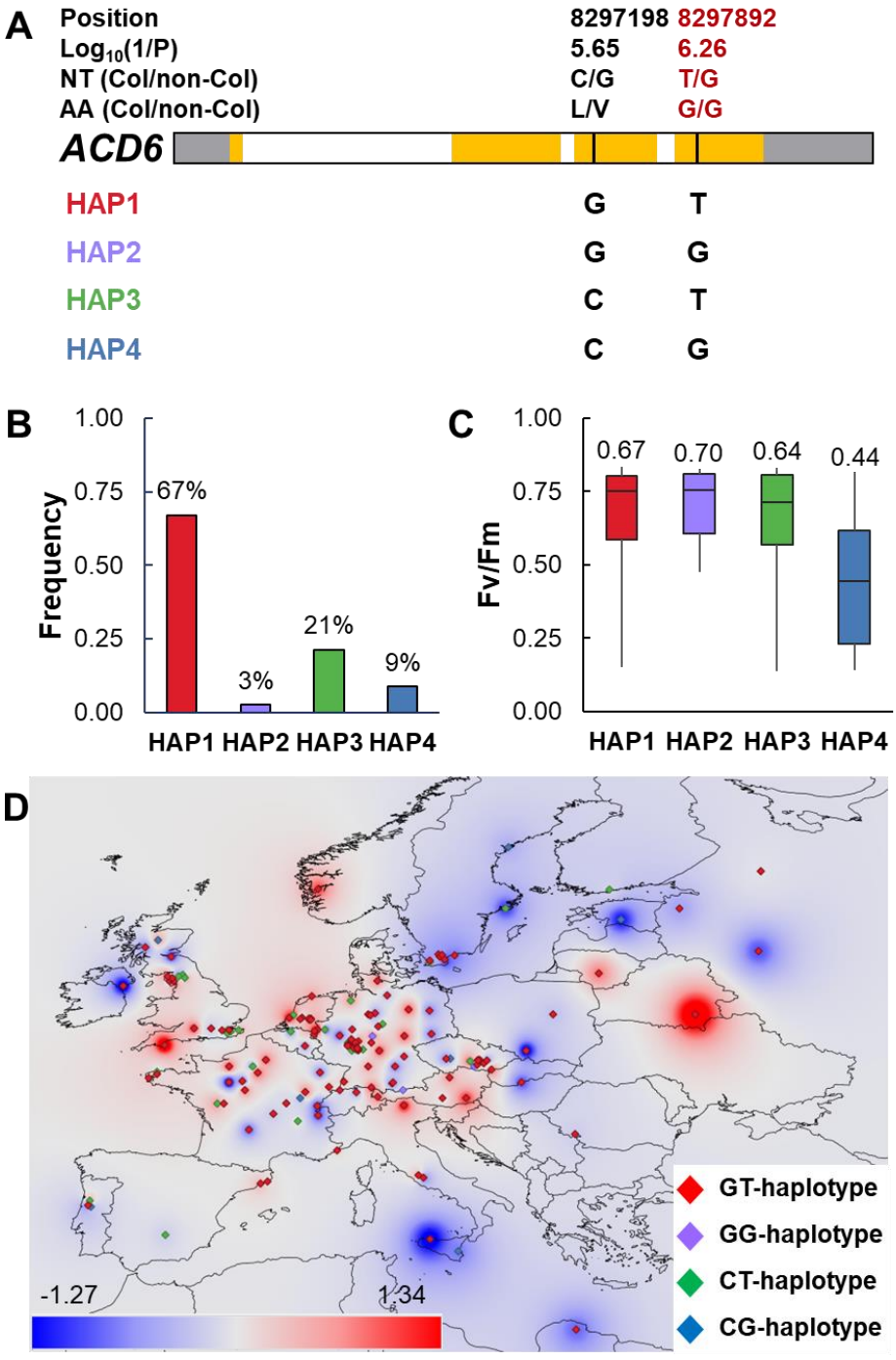

Figure 9. Geographic distribution and leaf senescence responses with respect to haplotypes of *ACD6*. (**A**), Schematic presentation of *ACD6* haplotypes. (**B**) Frequency of *ACD6* haplotypes among the examined accessions. (**C**) Senescence responses of accessions with different haplotypes. On the box plot middle lines are the mean and whiskers above and below the box indicate the 75th and 25th percentiles. (**D**) Geographical distribution of *ACD6* haplotypes. NT: nucleotide; AA: amino acid.

4.5. *ACD6* positively regulates age-induced but not dark-induced leaf senescence

Given the tight association between the *ACD6* locus with natural senescence responses and the enrichment of delayed senescence phenotypes in accessions with the 'T'-type SNP, I decided to investigate the biological functions of ACD6 protein in regulating leaf senescence. To achieve this, I evaluated senescence phenotypes in *ACD6* loss-of-function mutants of Col-0. Two independent T-DNA alleles, *acd6-2* and *acd6-11* were employed to avoid possible effects of unknown second mutations (**Figure 10**).

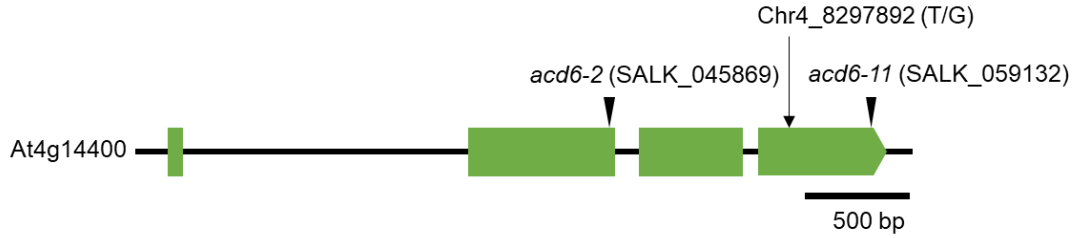

Figure 10. Characteristics of *acd6* mutants. Schematic representation of the *ACD6* gene, *At4g14400* and position of the T-DNA insert in the loss-of-function mutants, *acd6-2* and *acd6-11*.

I first examined the progression of age-induced leaf senescence in *acd6-2* and *acd6-11* by monitoring changes in morphological and physiological markers as well as the expression of senescence-associated genes (SAGs) (**Figure 11**). Color segmentation displayed leave green and yellow color ratio over the course of leaf age (**Figure 11A**). The photochemical efficiency in photosystem II and chlorophyll content gradually reduced as the leaves aged in all examined genotypes. However, the

reduction in both physiological and molecular markers in Col-0 was more evident compared with that in *acd6* mutants. Initially, visible color segmentation indicates a decreased proportion of leaf yellowing in *acd6-2* and *acd6-11* relative to Col during leaf aging (**Figure 11A**). At 34 DAE, the F_v/F_m value significantly reduced in Col-0 compared with that at 14 DAE (23%), while the reductions in *acd6-2* and *acd6-11* mutants were negligible (10% and 9%, respectively) (**Figure 11B**). Leaves of Col-0 also displayed lower chlorophyll content compared with *acd6* mutants, as indicated by higher yellowing percentage and lower vegetation index at 30 DAE and 34 DAE (**Figure 11C**,**D**). Similarly, age-induced expressions of well-known SAGs including *ORESARA1* (*ORE1*), *SAG12*, and *SAG29*, were significantly lower in both *acd6-2* and *acd6-11* relative to Col-0 (**Figure 11E**,**F**,**G**). These results indicate that both *acd6* mutants displayed delayed senescence phenotypes and *ACD6* functions as a positive regulator in age-induced leaf senescence. Interestingly, *ACD6* may not be involved in plant dark-induced senescence response. After dark incubation, there was no significant difference between Col-0, *acd6-2*, and *acd6-11* mutants under the same conditions for the examined parameters, including photochemical efficiency in photosystem II (F_v/F_m) and chlorophyll content (**Figure 12**). This finding indicates that although age- and dark-induced senescence processes may share common pathways, distinct pathways for each process also exist and *ACD6* may function specifically in age-induced leaf senescence.

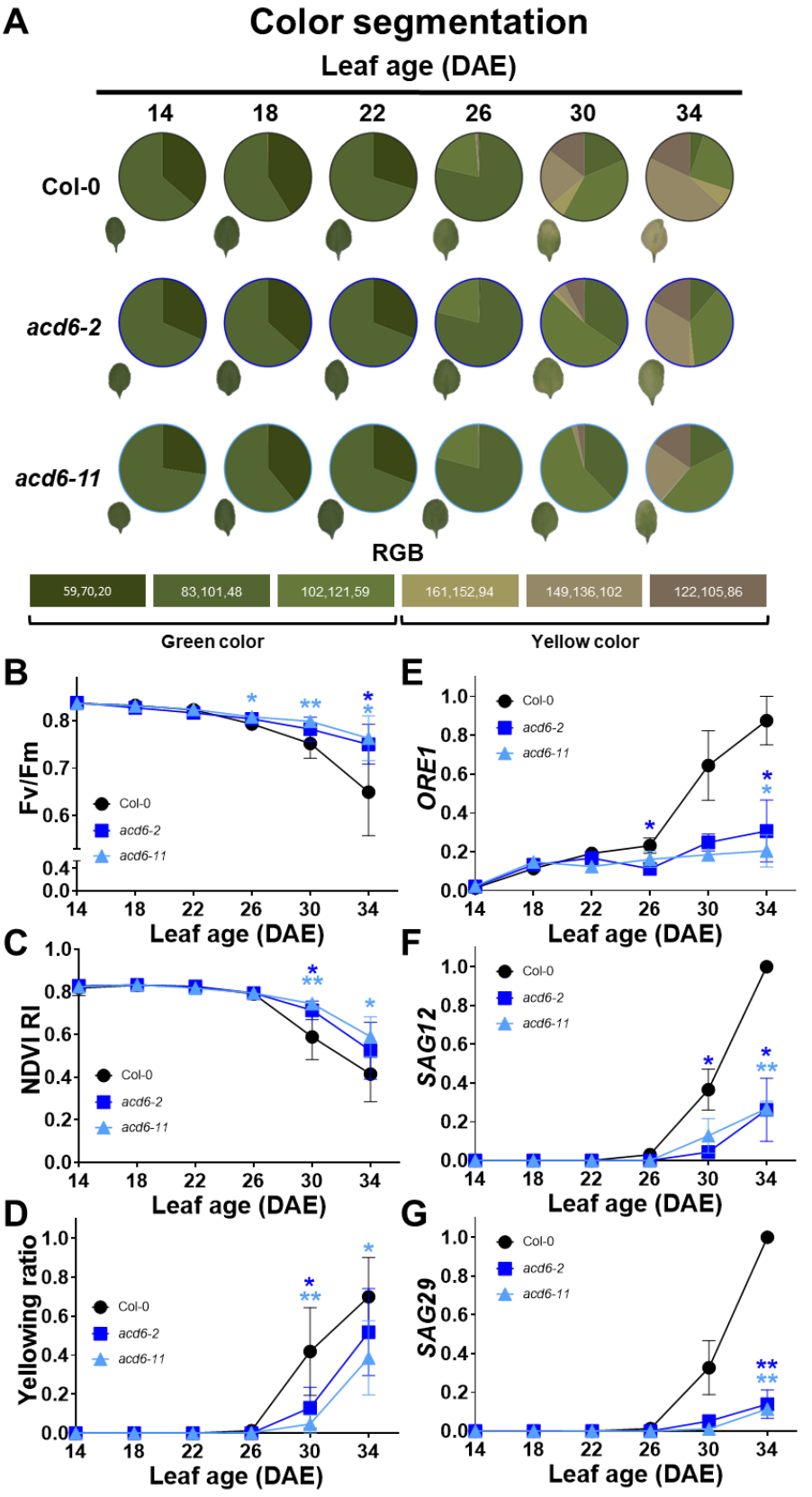

Figure 11. **Physiological and molecular response of *acd6* mutants in age-induced leaf senescence.** (**A**,**B**,**C**,**D**) Pie chart with color segmentation (**A**) and changes in physiological indexes including F_v/F_m (**B**), NDVI RI (**C**), and proportion of yellow color (**D**) in *acd6-2* and *acd6-11* leaves during age-induced leaf senescence. Data were normalized with values of the same accessions or genotypes at 14 DAE. (E,F,G) Expression of senescence-associated genes *ORE1* (**E**), *SAG12* (**F**), and *SAG29* (**G**) in *acd6-2* and *acd6-11* leaves during age-induced leaf senescence. The results are shown as the mean ± 95% CI of four experiments. Statistical analysis was performed using Student's *t*-test: *, P<0.05; **, P<0.01.

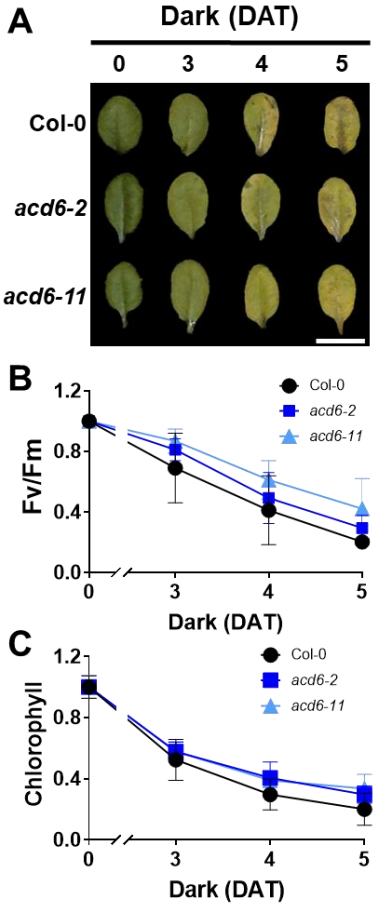

Figure 12. Dark-induced senescence response in *acd6* mutants. (**A**) Representative visible image of the 3rd and 4th leaves of Col-0 and *acd6* mutants in dark-induced senescence. Bar: 1 cm. (**B** and **C**) Changes in physiological indexes: F_v/F_m (**B**) and chlorophyll contents (**C**) in Col-0 and *acd6* mutants during dark-induced leaf senescence. The results are shown as the mean ± 95% CI (n = 6) from two independent experiments.

4.6. Variation of natural senescence responses is associated with an SNP in *ACD6*

The most significant SNP associated with natural variation in senescence phenotypes of Arabidopsis accessions is located at nucleotide 8,297,892 on chromosome 4 in the *ACD6* coding sequence (**Figure 7**). Based on the phenomic evaluation of age-induced leaf senescence, the examined accessions in this study were divided into two groups, early and delayed senescence. The inconsistency between age-induced and dark-induced senescence phenotypes of Arabidopsis natural accessions can be observed (**Figure 13**), which further indicates the differences between age-induced and dark-induced leaf senescence in natural populations. I found an enrichment of delayed senescence phenotypes in accessions with the 'T'-type SNP. On the other hand, early senescence accessions contain both 'T'-type and 'G'-type SNP (**Figure 13**). Therefore, I tried to address the functional extents of the *ACD6* gene in regulating leaf senescence. For this purpose, I used CRISPR/Cas9 genome editing to generate *ACD6* loss-of-function mutants in different Arabidopsis accessions with early and delayed senescence phenotypes (**Table 2**, **Figure 14**). Data were normalized with values of the same accessions or genotypes at 14 DAE. The F_v/F_m values of two early senescence accessions Mz-0 and Est-1 significantly reduced at 26 DAE compared to that of 14 DAE (73% and 57%, respectively) while Col maintained a relatively high level at the same time (91%) (**Figure 14B**). On the other hand, photochemical efficiency of the delayed senescence accessions Bur-0 and Kin-0 sustained at leaf aged (82% and 79% at 30 DAE; 61% and 52% at 34 DAE, respectively) when Col photosynthetic activities were seriously disrupted (60% at 30 DAE and 24% at 34 DAE) (**Figure 14G**). Other tested parameters, including

chlorophyll contents and expression of the senescence-associated genes (SAGs) *ORE1* and *SAG12*, also yielded consistent results (**Figure 14C**,**D**,**E**,**H**,**I**,**J**).

Table 2. The list of *acd6* gene-editing mutants in accession showing diverse senescence symptoms

Accession	Senescence phenotype in accession	Haplotype	Allele and name	Mutation
Col-0	-	HAP3	*acd6-21*_Col-0	'A' insertion
Mz-0	Early	HAP4	*acd6-22*_Mz-0	'C' insertion
Est-1	Early	HAP4	*acd6-23*_Est-1	'G' insertion
Bur-0	Delay	HAP1	*acd6-25*_Bur-0	Deletion of 8 nucleic acids
Kin-0	Delay	HAP3	*acd6-26*_Kin-0	'A' insertion

*Note: Haplotype information of accessions was derived from **Figure 9**

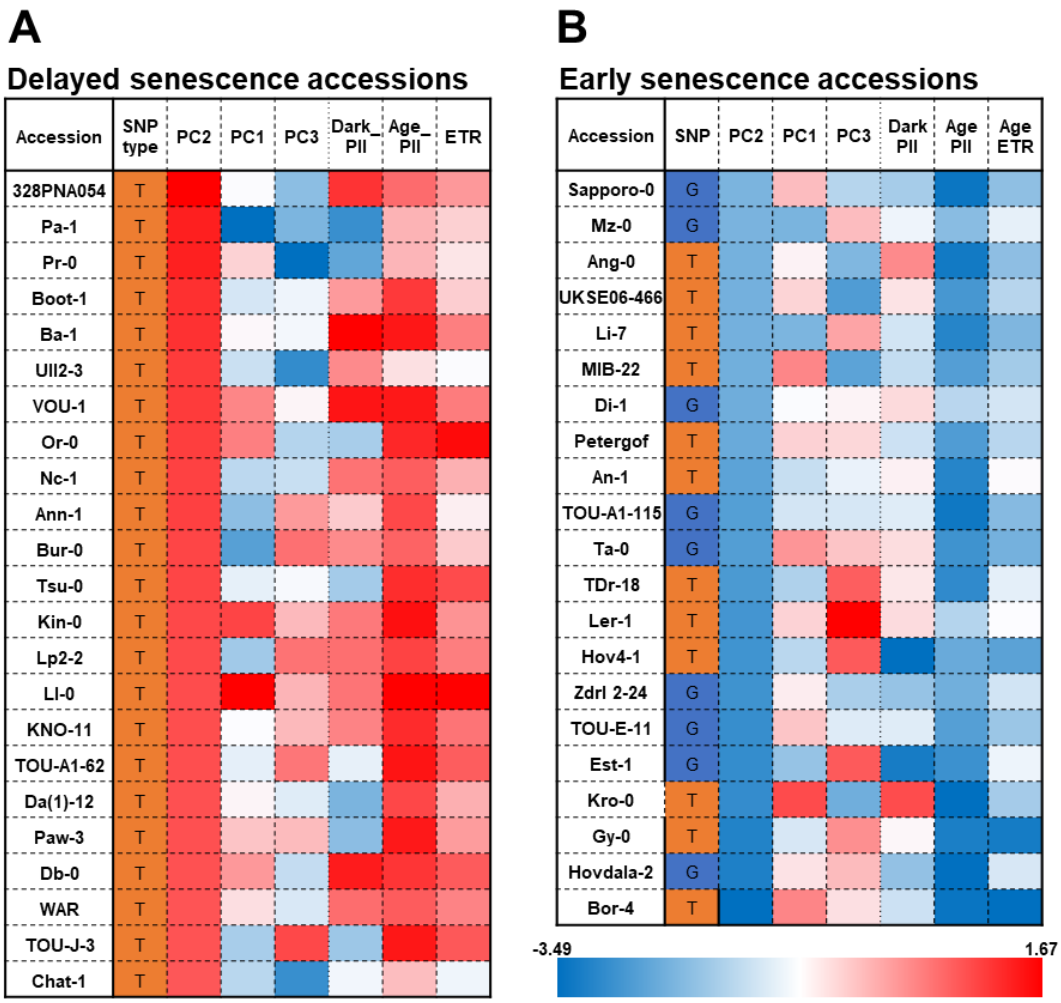

Figure 13. Diverse age-induced senescence symptoms and *ACD6* variants from early and delayed leaf senescence accessions. (**A**) and (**B**) Lists of representative delayed (**A**) and early (**B**) leaf senescence accessions were determined by phenomic evaluation of leaf senescence. Dark PSII and Age PSII, photochemical efficiency of photosystem II during dark- and age-induced senescence, respectively; ETR, ETR during age-induced senescence. SNP type, the SNP with the highest association with PC2 in *ACD6*.

All examined *acd6* mutants displayed delayed senescence responses compared to their respective backgrounds (**Figure 14**). However, the extents of delay are different among accessions. Two-way ANOVA analyses confirmed that the interaction between leaf age and plant genotype significantly affected plant photochemical efficiency and chlorophyll content in both early and delayed senescence accessions (p-value < 0.001)

(**Figure 15A**,**B**,**E**,**F**). Loss-of-function of *ACD6* in the early senescence backgrounds significantly delayed plant age-induced senescence responses. At 30 DAE, the effect of knocking out *ACD6* on plant photochemical efficiency was significantly higher in Mz-0 and Est-1 compared to that in Col-0 (99% in *acd6-21*_Col-0 versus 60% in Col-0, 97% in *acd6-22*_Mz-0 versus 8% in Mz-0; 87% in *acd6-23*_Est-1 versus 25% in Est-1) (**Figure 14B**; **Figure 15C**). Similarly, inhibition of *ACD6* function in Mz-0 and Est-1 resulted in better chlorophyll preservation (**Figure 14A**,**C**; **Figure 15D**). Expression analysis of well-known senescence-associated genes also provided consistent results (**Figure 14D**,**E**). The extension of leaf longevity in *acd6-22*_Mz-0 and *acd6-23*_Est-1 was even more evident at 34 DAE. While 34-day-old leaves of Mz-0 and Est-1 were already dead, 34-day-old leaves of *acd6-22*_Mz-0 and *acd6-23*_Est-1 still maintained relatively high levels of photochemical efficiency (96% and 78% respectively) and chlorophyll content (64% and 57%, respectively) (**Figure 14A**,**B**,**C**). In contrast with early senescence accessions, loss-of-function of *ACD6* in delayed senescence accessions did not display the same level of effect (**Figure 15G**,**H**). Compared to Col-0 at 30 DAE, the enhancement of photochemical efficiency caused by the inhibition of *ACD6* function in Bur-0 and Kin-0 was significantly lower (99% in *acd6-21*_Col-0 versus 60% in Col-0, 80% in *acd6-25*_Bur-0 versus 61% in Bur-0; 87% in *acd6-26*_Kin-0 versus 53% in Kin-0) (**Figure 14G**; **Figure 15G**). Consistently, chlorophyll content and expression of senescence-associated genes indicated the lower effects of *ACD6* inhibition in delayed senescence accessions in comparison with that in Col-0 (**Figure 14H**,**I**,**J**; **Figure 15H**). These results indicate

that *ACD6* may be hyperactive in early senescence accessions, and thus might contribute to the early responses of age-induced leaf senescence in these accessions.

Regarding dark-induced leaf senescence, loss-of-function of *ACD6* did not show any effects on plant senescence phenotypes. *acd6* mutants displayed comparable levels of photochemical efficiency and chlorophyll contents with their respective background after dark incubation (p-value > 0.05) (**Figure 16**). These results further confirm my observation that *ACD6* specifically regulates age-induced leaf senescence in Arabidopsis.

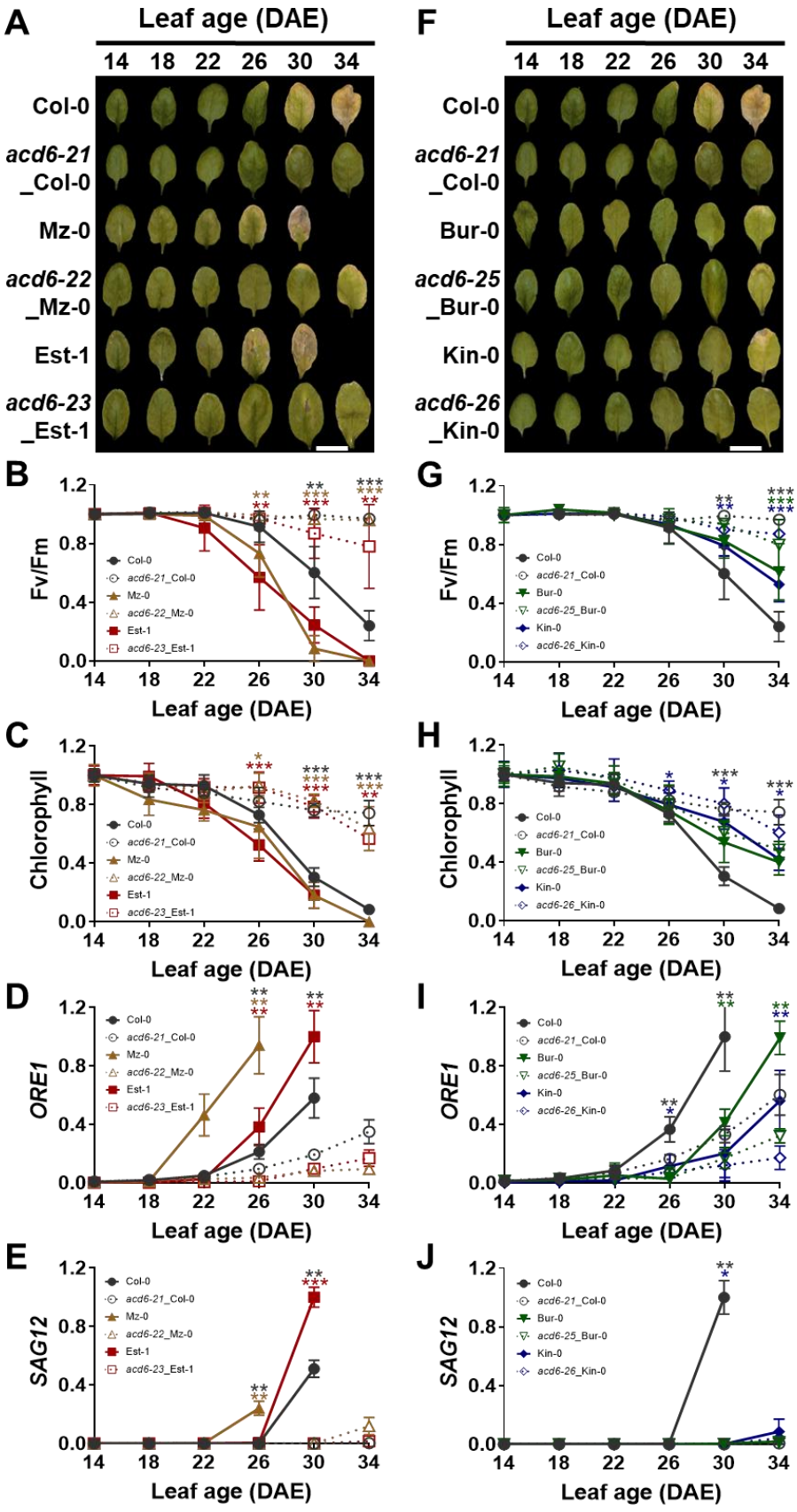

Figure 14. **Age-induced senescence responses in *acd6*-KO mutant in the early and delayed leaf senescence accessions.** (**A**-**J**) physiological and molecular evaluation of age-induced leaf senescence responses in *acd6*-KO mutants in the backgrounds of early (**A**-**E**) and delayed (**F**-**J**) leaf senescence accessions. (**A**,**F**) Visible image of the representative 3rd and 4th leaves of WT and *acd6* mutant in accessions in age-induced leaf senescence. Bars: 1 cm (**B**,**C** and **G**,**H**) Changes in physiological indexes (F_v/F_m, and Chlorophyll contents) in WT and *acd6* mutants in accessions in age-induced leaf senescence. Data were normalized with values of the same accessions or genotypes at 14 DAE. The results are shown as the mean ± 95% CI (n = 6 to 12) of two experiments. (**D**,**E** and **I**,**J**) Expression of senescence-associated genes (*ORE1* and *SAG12*) along aging. The transcript abundance of each gene was analyzed by qRT-PCR, normalized to *UBQ10*. Data in (**D**,**E** and **I**,**J**) are shown as means ± 95% CI (n = 2). Statistical analysis was performed using Student's t-test to compare *acd6*-KO mutants and their respective backgrounds at the same age: *, P<0.05; **, P<0.01; ***, P<0.001. All plants of 10 genotypes from this experiment were grown and harvested at the same time. The two groups presented in this figure were for presentation purposes only and the same set of leaves of Col-0 and *acd6-21*_Col-0 were used for both groups.

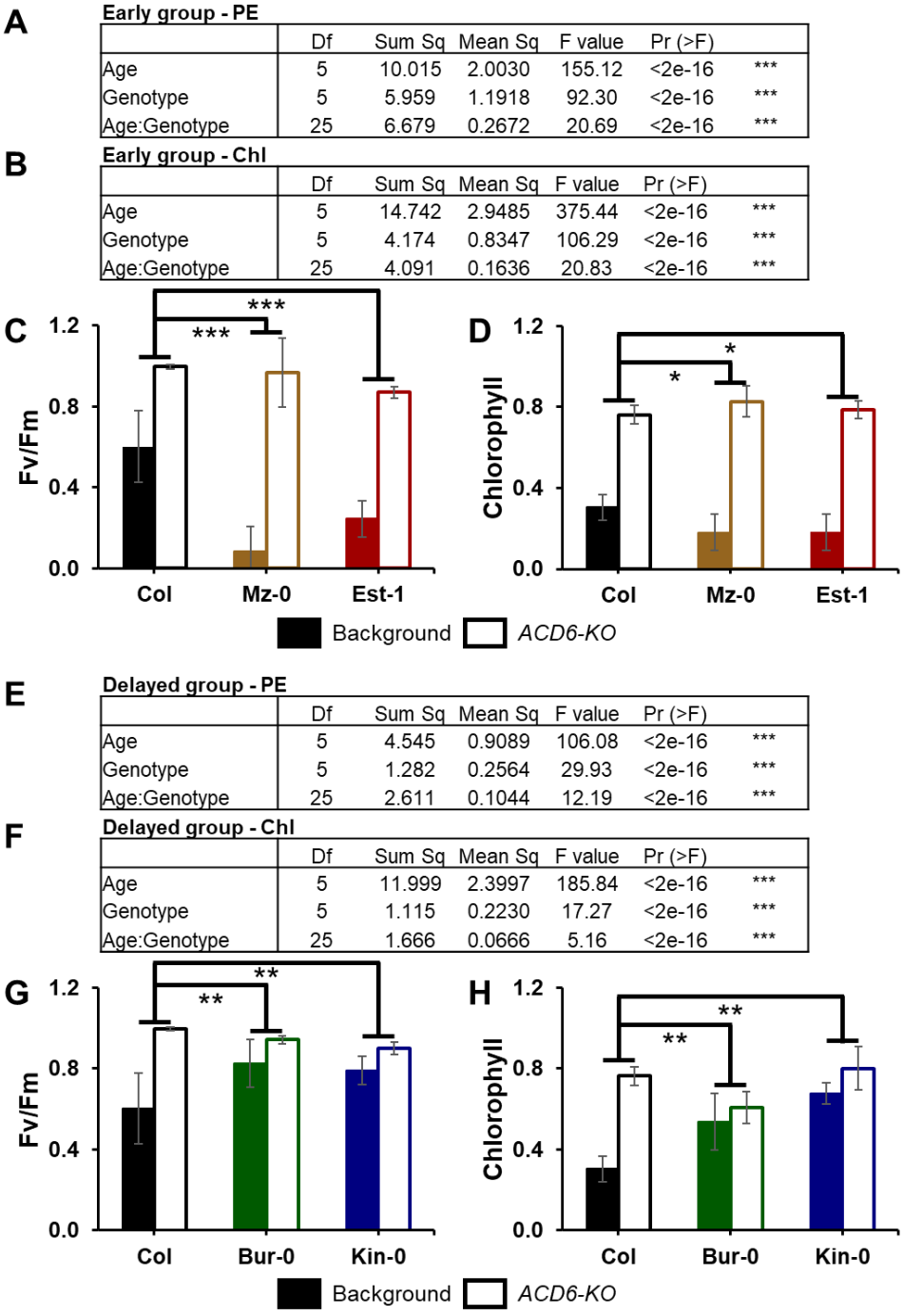

Figure 15. Statistical analyses for age-induced senescence responses in *acd6*-KO mutants in the early and delayed leaf senescence accessions. (**A**,**B** and **E**,**F**) Two-way ANOVA analyses for the effects of the interaction between leaf age and plant genotype on leaf photochemical efficiency and chlorophyll contents. (**C**,**D** and **E**,**F**) Representative F_v/F_m and chlorophyll contents of leaves at 30 DAE in early and delayed senescence accessions. The results are shown as the mean ± 95% CI. Contrast

analyses were conducted to compare the effects of knocking out *ACD6* on different accessions. *, P<0.05; **, P<0.01; ***, P<0.001.

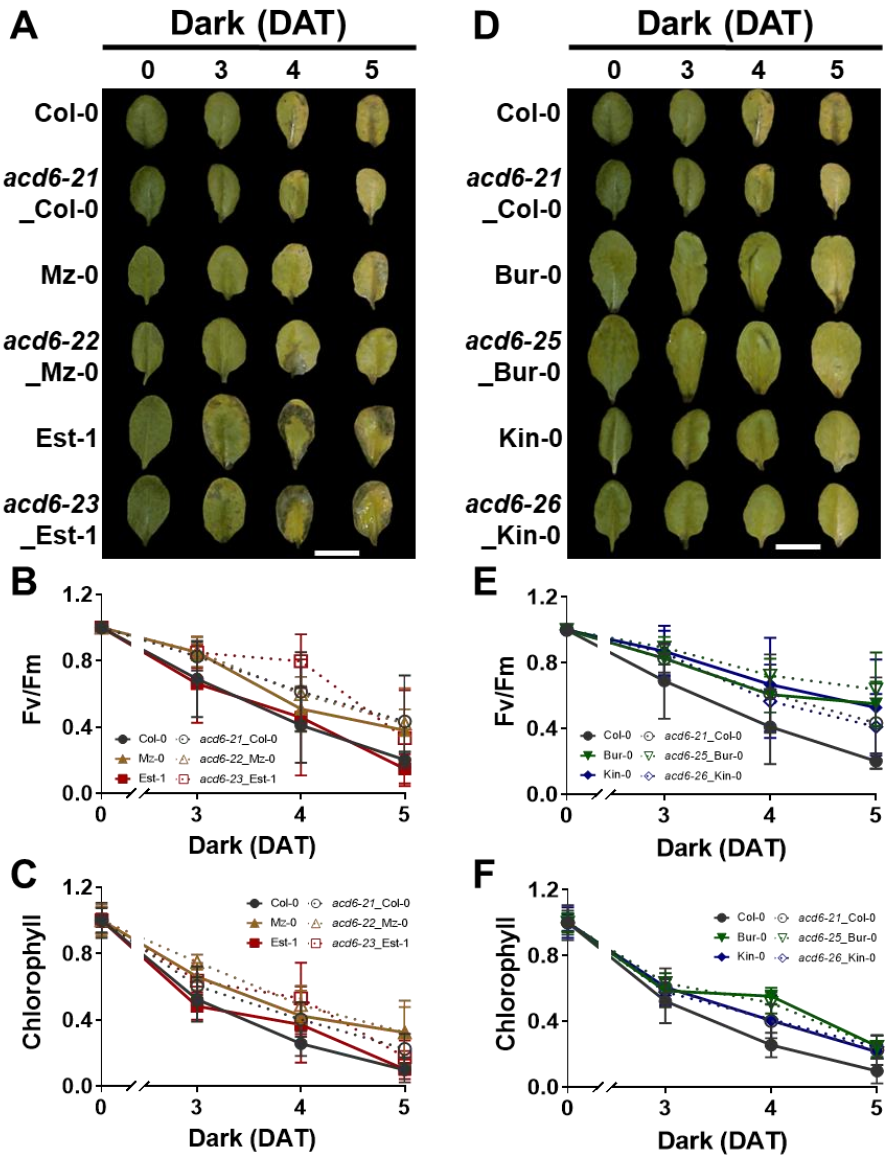

Figure 16. Dark-induced senescence responses in *acd6*-KO mutant in the early and delayed leaf senescence accessions. Representative visible image (**A** and **B**) and changes in chlorophyll contents (**C** and **D**) of the 3rd and 4th leaves of Col-0 and *acd6*-KO mutants in the backgrounds of early (**A** and **C**) and delayed (**B** and **D**) accessions during dark-induced senescence. Bar: 1 cm. The results are shown as the mean ± 95% CI (n = 6) of two independent experiments.

4.7. *ACD6* functions in SA-induced leaf senescence

Given previous lines of evidence that *ACD6* is involved in the SA signaling pathway in response to various stimuli (Todesco et al., 2014, Pluharova et al., 2019), I was also interested in investigating the functional roles of this ankyrin protein in SA-induced leaf senescence. I first examined the senescence responses of Col-0 and various *acd6* mutants in Col-0 under different SA concentration treatments (1.2 mM and 2.4 mM) (**Figure 17**). I normalized data with values of the same genotypes at 0 DAT. The examined *acd6* mutants include the CRISPR/Cas9 gene-edited mutant *acd6-21*_Col-0, the gain-of-function mutant *acd6-1*, and the T-DNA insertion mutants *acd6-2*. The gain-of-function mutant *acd6-1* displayed early senescence phenotypes compared to Col-0 under both SA concentrations (**Figure 17**). Under 1.2 mM SA treatment, F_v/F_m and chlorophyll content of *acd6-1* were significantly lower than that of Col-0 at 4 DAT (54% versus 68% for F_v/F_m and 32% versus 54% for chlorophyll content, *p*-value < 0.01) and 6 DAT (30% versus 46% for F_v/F_m and 5% versus 14% for chlorophyll content, *p*-value < 0.01) (**Figure 17B**,**C**). Consistent results were obtained from leaves under 2.4 mM SA treatment, though only F_v/F_m value displayed significant differences between *acd6-1* and Col-0 (18% versus 30% at 4 DAT, p< and 11% versus 26% at 6 DAT, *p*-value < 0.05) (**Figure 17E**,**F**). Interestingly, knocking out *ACD6* was not very effective in altering plant SA-induced senescence responses. Though displayed slightly delayed senescence phenotypes, the differences in F_v/F_m and chlorophyll content values between the loss-of-function mutants *acd6-21*_Col-0 and *acd6-2* with Col-0 were insignificant under most of the treatment conditions (**Figure 17**). Particularly, among the examined parameters, only chlorophyll content

of *acd6-21*_Col-0 and *acd6-2* under 1.2 mM SA treatment were significantly higher than that of Col-0 (41% and 27% respectively versus 14% at 6 DAT, *p*-value < 0.05) (**Figure 17C**).

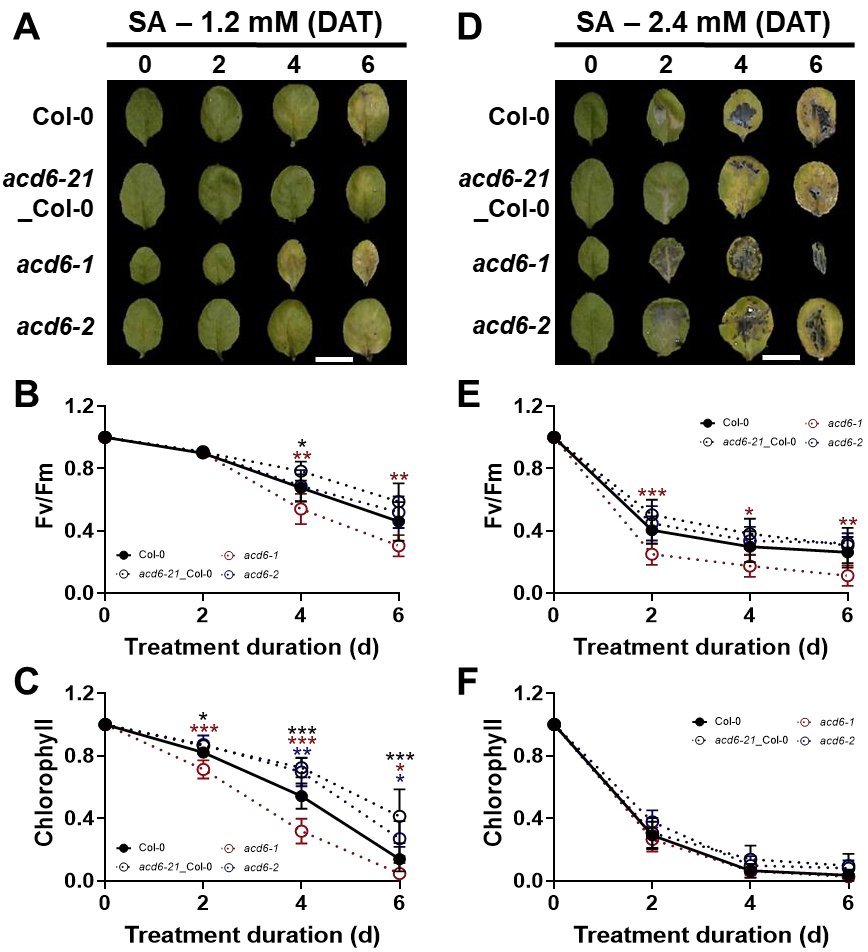

Figure 17. Senescence responses of *acd6* mutants treated under different salicylic acid (SA) concentrations. (**A**,**D**) Visible image of the representative third and fourth leaves of Col-0 and *acd6* mutants in SA-induced leaf senescence. Bars: 1 cm (**B**,**C** and **E**,**F**) Changes in physiological indexes (F_v/F_m, and Chlorophyll contents) in Col-0 and *acd6* mutants in SA-induced leaf senescence. Data were normalized with values of the same accessions or genotypes at 0 DAT. The results are shown as the mean ± 95% CI (n = 24). Statistical analysis was performed using Student's *t*-test to compare between *acd6* mutants and Col-0 at the same treatment duration: *, P<0.05; **, P<0.01; ***, P<0.001.

As *ACD6* functions in age-induced leaf senescence in an accession-dependent manner (**Figure 14**, **Figure 15**), I was also interested in investigating the functional differences of *ACD6* in SA-induced leaf senescence among Arabidopsis natural accessions. I employed the same set of genotypes as were used in the previous results, including the backgrounds with different senescence phenotypes and their respective *ACD6* loss-of-function mutants (**Table 1**). The 3rd and 4th leaves of 3-week-old plants were harvested and incubated in MES buffer supplied with 2.4 mM SA solution under the growth room condition. Data were normalized with values of the same accessions or genotypes at 0 DAT. The obtained results revealed interesting insight regarding the functional roles of *ACD6* in SA signaling and senescence pathway. Inconsistent with the obtained results from my previous senescence assays, the effects of SA treatment on senescence responses varied among accessions independent of their age-induced senescence phenotypes (**Figure 18**). After 6 days of SA treatment, the photochemical efficiency of the plants was 26%, 21%, 43%, 43% and 35% of those at 0 DAT for Col-0, Est-1, Mz-0, Bur-0 and Kin-0, respectively (**Figure 18**). Similarly, chlorophyll content displayed an inconsistent trend compared to age-induced leaf senescence (**Figure 18**).

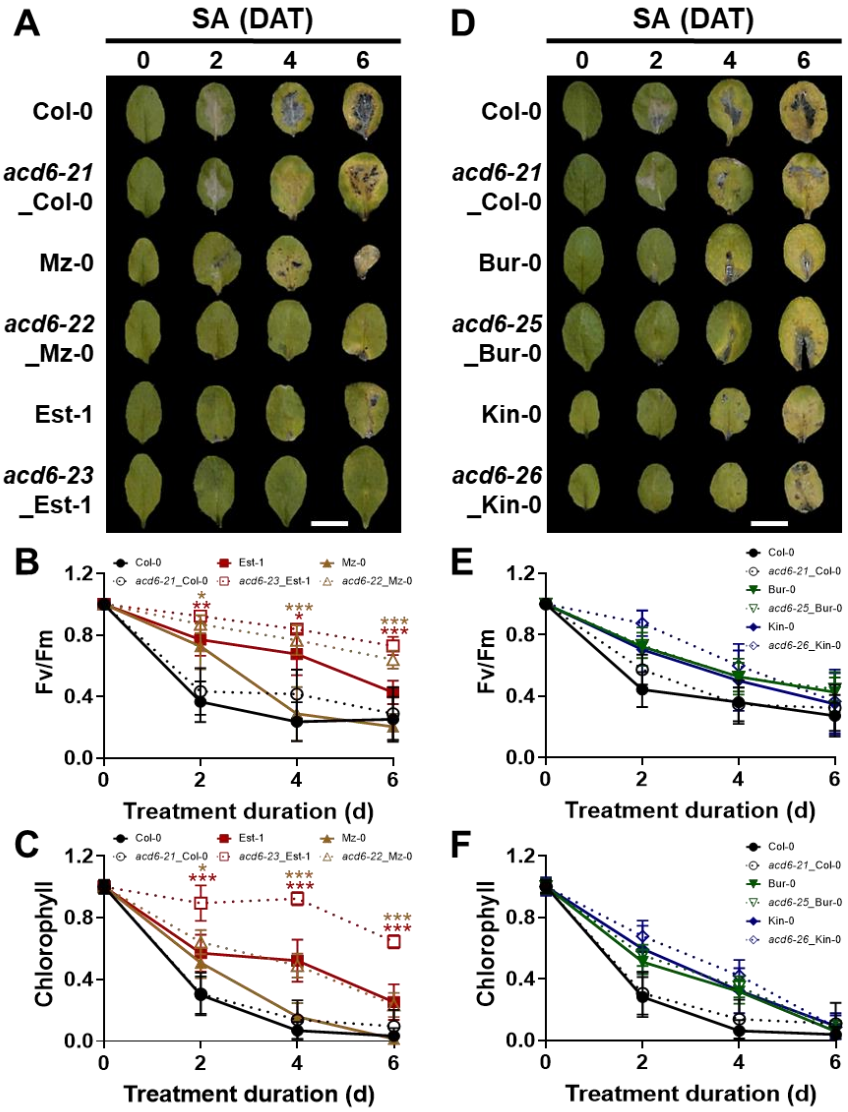

Figure 18. **Salicylic acid (SA)-induced senescence responses in *acd6*-KO mutant in the early and delayed leaf senescence accessions.** (**A**-**F**) physiological evaluation of SA-induced leaf senescence responses in *acd6*-KO mutants in the backgrounds of early (**A**-**C**) and delayed (**D**-**F**) leaf senescence accessions. (**A**,**D**) Visible image of the representative 3rd and 4th leaves of WT and *acd6* mutant in accessions in SA-induced leaf senescence. Bars: 1 cm (**B**,**C** and **G**,**H**) Changes in physiological indexes (F_v/F_m, and Chlorophyll contents) in WT and *acd6* mutants in accessions in SA-induced leaf senescence. Data were normalized with values of the same accessions or genotypes at 0 DAT. The results are shown as the mean ± 95% CI (n = 12). Statistical analysis was performed using Student's *t*-test to compare *acd6*-KO mutants and their respective backgrounds at the same treatment duration: *, P<0.05; **, P<0.01; ***, P<0.001.

Knocking out *ACD6* repressed the effects of SA on senescence responses of all examined accessions (**Figure 18**). However, similar to age-induced leaf senescence, the effects also varied among the backgrounds. The significant effects of the interaction between treatment duration and plant genotype on F_v/F_m value and chlorophyll contents were confirmed by two-way ANOVA (*p*-value < 0.001) (**Figure 19A**,**B**,**E**,**F**). The disrupted function of *ACD6* in the early senescence accessions evidently delayed leaf senescence under SA treatment. At 6 DAT, F_v/F_m values of *acd6-22*_Mz-0 and *acd6-23*_Est-1 were significantly higher than those of their respective backgrounds (64% in *acd6-22*_Mz-0 versus 21% in Mz-0; 73% in *acd6-23*_Est-1 versus 43% in Est-1, *p*-value < 0.001) (**Figure 18**). Chlorophyll content yielded consistent results in the *ACD6* loss-of-function mutants of these accessions (**Figure 18**). In contrast, ACD6 in Col-0 and the delayed senescence accessions do not seem to play important roles in SA-induced leaf senescence. After 6 days of SA treatment, *acd6-21*_Col-0, *acd6-25*_Bur-0, and *acd6-26*_Kin-0 displayed similar responses compared to the backgrounds in both photochemical efficiency (32% in *acd6-21*_Col-0 versus 27% in Col-0, 45% in *acd6-25*_Bur-0 versus 43% in Bur-0; 37% in *acd6-26*_Kin-0 versus 35% in Kin-0, *p*-value > 0.05) and chlorophyll content (8% in *acd6-21*_Col-0 versus 4% in Col-0, 8% in *acd6-25*_Bur-0 versus 6% in Bur-0, 9% in *acd6-26*_Kin-0 versus 9% in Kin-0, *p*-value > 0.05) (**Figure 18**). The effects of knocking out *ACD6* on plants photochemical efficiency and chlorophyll contents were also significantly higher in early senescence accessions compared to that in Col-0 and delayed senescence accessions (*p*-value < 0.05) (**Figure 19C**,**D**,**G**,**H**). These data suggest that the functional variation of *ACD6* is also present in SA-induced leaf

senescence and *ACD6* may serve as an integrator between the SA signaling pathway and age-induced leaf senescence. Overall, my obtained data suggest that natural variations in senescence responses of Arabidopsis may be on account of *ACD6* function and studying in detail the *ACD6* structure and function in accessions will provide more insight into the evolutionary and adaptive roles of leaf senescence.

A Early group - PE

	Df	Sum Sq	Mean Sq	F value	Pr (>F)	
Duration	3	20.800	6.9330	353.55	<2e-16	***
Genotype	7	9.891	1.4130	72.06	<2e-16	***
Duration:Genotype	21	5.178	0.2470	12.57	<2e-16	***

B Early group - Chl

	Df	Sum Sq	Mean Sq	F value	Pr (>F)	
Duration	3	37.82	12.6070	956.36	<2e-16	***
Genotype	7	11.04	1.5670	119.59	<2e-16	***
Duration:Genotype	21	4.75	0.2260	17.14	<2e-16	***

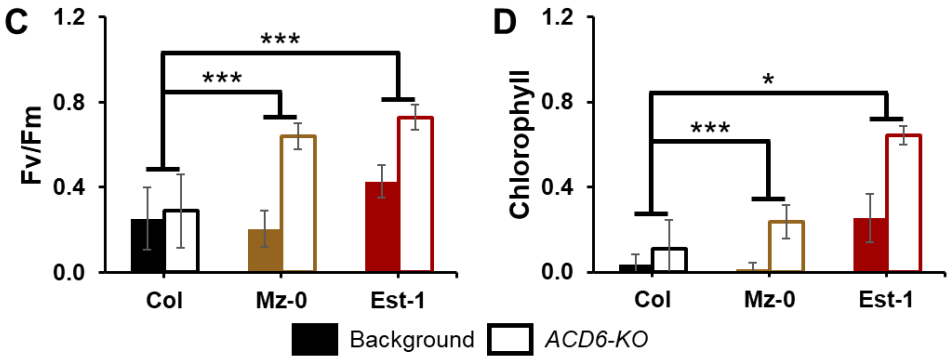

E Delayed group - PE

	Df	Sum Sq	Mean Sq	F value	Pr (>F)	
Duration	3	28.210	9.4030	328.19	<2e-16	***
Genotype	7	5.233	0.7480	26.09	<2e-16	***
Duration:Genotype	21	3.457	0.1650	5.75	<2e-16	***

F Delayed group - Chl

	Df	Sum Sq	Mean Sq	F value	Pr (>F)	
Duration	3	47.840	15.9460	1129.05	<2e-16	***
Genotype	7	2.090	0.2980	21.10	<2e-16	***
Duration:Genotype	21	1.860	0.0880	6.26	<2e-16	***

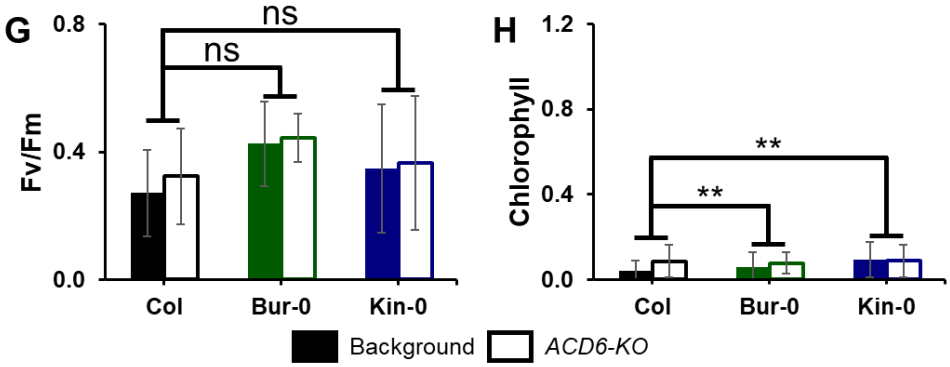

Figure 19. Statistical analyses for salicylic acid (SA)-induced senescence responses in *acd6*-KO mutants in the early and delayed age-induced leaf senescence accessions. (**A**,**B** and **E**,**F**) Two-way ANOVA analyses for the effects of the interaction between leaf age and plant genotype on leaf photochemical efficiency and chlorophyll contents. (**C**,**D** and **E**,**F**) Representative F_v/F_m and chlorophyll contents of leaves at 6 DAT in early and delayed senescence accessions. The results are shown as the mean ± 95% CI. Contrast analyses were conducted to compare the

effects of knocking out *ACD6* on different accessions. *, P<0.05; **, P<0.01; ***, P<0.001.

5. DISCUSSION

In this study, I applied the phenome high-throughput investigator (PHI) to investigate the age-induced leaf senescence responses among a large collection of Arabidopsis natural accessions (**Figure 3**). I employed principal component (PC) analysis to reduce the dimensionality of the extracted data and identify biologically meaningful PC factors that can represent a group of phenomic traits related to the current senescence stage of the leaves (**Figure 5**). Combining my obtained PC values with prior information from independent datasets, I can better explain the correlation of leaf senescence with environmental factors and physiological traits (**Figure 6**). I was able to identify several external and physiological factors that are tightly correlated with leaf senescence phenotypes, such as humidity and temperature (**Figure 6A**) or defense, flowering, and ion contents (**Figure 6B**). Furthermore, I discovered a genetic locus responsible for the divergence of natural senescence programs (**Figure 7**), which encodes for *ACCELERATED CELL DEATH 6* (*ACD6*). Notably, *ACD6* appears to function specifically in age-induced leaf senescence (**Figure 11**), and its functional extent varies among accessions with different senescence phenotypes (**Figure 14**). My obtained results also indicated that *ACD6* may regulate age-induced leaf senescence via the SA signaling pathway, as its functional variation among natural accessions is also presented in SA-induced leaf senescence (**Figure 18, Figure 20**).

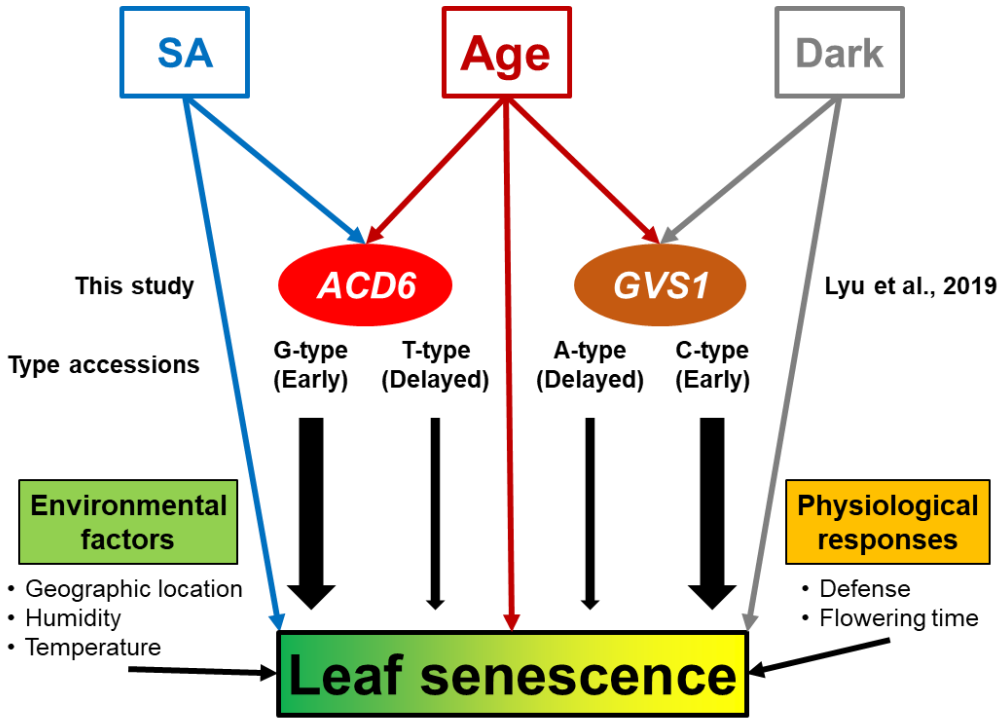

Figure 20. Schematic model represent the regulatory factors of leaf senescence in Arabidopsis natural accessions. Various environmental and physiological factors that can affect plant senescence responses including geographical location, humidity and temperature or defense and flowering time. *GVS1* was found to function in age- and dark-induced senescence in accession-dependent manners (Lyu et al., 2019). On the other hand, the functional diversity of *ACD6* alleles only present in age- and SA-induced leaf senescence.

Previously, the phenotypic evaluation of senescence responses was mainly based on single traits such as F_v/F_m or chlorophyll contents. However, senescence is a complex trait that is regulated by both genetic and environmental factors. Leaf senescence phenotypes result from the combination of multiple physiological and biochemical traits, which may not be completely described by individual qualitative or quantitative variables (Goddard et al., 2016). This pleiotropic characteristic suggests that senescence should be evaluated in a holistic approach, in which various relevant phenotypic traits need to be taken into account. This led to the demand for high-dimensional phenotypic data, referring to multivariate phenotypic variables that are

used to describe a particular phenotype (Collyer et al., 2015). Accordingly, multiple high-throughput phenotyping systems have been developed. My study employed the PHI, a high-throughput phenotyping platform, to obtain various senescence-related traits for comprehensively evaluating leaf phenotypes during senescence process (**Figure 3**). By using the PC analysis, I was able to identify meaningful biological values that represent senescence phenotypes of different Arabidopsis natural accessions (**Figure 5**). My approach using high-dimensional phenotypic data and principal component (PC) analysis provides a comprehensive evaluation of the leaf phenotype during senescence compared to the single trait-based approach.

To date, numerous attempts to investigate senescence programs in Arabidopsis natural populations have been conducted. However, these studies still have limitations. There have been no attempts to study age-induced functional leaf senescence responses in natural accessions (Lyu et al., 2019). Previous studies only focused on dark-induced leaf senescence. Dark treatment in detached leaves has been widely used to study age-induced senescence (Weaver and Amasino, 2001). Dark- and age-induced leaf senescence programs were also indicated to have partially shared mechanisms, as numerous functional SAGs such as *ORE9* (Woo et al., 2001), *NAC029* (Guo and Gan, 2006) or *NAC092* (Kim et al., 2009) have been found to function in both pathways. However, dark-induced leaf senescence responses are largely based on artificial starvation, which differs from age-induced leaf senescence programs (Buchanan-Wollaston et al., 2005). Compared to the synchronous symptoms throughout the leaf by dark treatment, age-induced leaf senescence often starts gradually from the tip to the base. Furthermore, the fast progression of dark-induced leaf senescence compared

to developmental senescence may overwhelm anti-senescence activity, another important aspect of senescence programs. Transcriptomic analyses in Arabidopsis also revealed significant differences in molecular responses between natural senescing leaves and detached dark-held leaves (Buchanan-Wollaston et al., 2005; Breeze et al., 2011). Consistently, my obtained data have indicated the differences between age-induced and dark-induced leaf senescence in Arabidopsis natural accessions, whether it is phenotypes (**Figure 4**, **Figure 8**) or correlation with other factors (**Figure 6**).

Senescence is a highly controlled degenerative process that is influenced by various internal and external factors (Zhang et al., 2021). The correlation tests of my obtained PC values with multiple environmental and physiological variables revealed some interesting insights. Among the examined environmental factors, senescence phenotypes were significantly associated with humidity and temperature (**Figure 6A**). High/low temperature and water deficit are major abiotic stresses that directly restrict plant growth and promote leaf senescence. Previous studies have shown that senescence responses and abiotic stress tolerance often being altered together in transgenic plants, such as *AtMYBL*-overexpressing Arabidopsis (Zhang et al., 2011) or *AtERF019*-overexpressing Arabidopsis (Scarpeci et al., 2017). Furthermore, geographical location also highly affected leaf senescence responses in Arabidopsis natural accessions (**Figure 6A**). Latitude and longitude affect several aspects of climate such as the amount of solar radiation, day length or wind conditions, which directly contribute to the regulation of leaves growth and development. Overall, my results further imply the critical roles of external conditions in shaping plant

senescence responses, as well as indicate the adaptive roles of senescence for plants in their natural habitats.

Senescence was previously found to be closely associated with various morphological and life history traits such as flowering time (Levey and Wingler, 2005). In this study, response to diverse pathogens and bacteria as well as flowering-related traits also correlated with senescence in accessions (**Figure 6B**), which is in agreement with previous results. Age-induced leaf senescence and defense response programs have been indicated to share common regulations in several studies. Transcriptomic analyses revealed the enrichment of gene ontology in terms of autophagy, immune response, defense response, and response to reactive oxygen species, suggesting a molecular relationship between defense and leaf senescence (Breeze et al., 2011; Buchanan-Wollaston et al., 2005; van de Graaf et al., 2006). Various genes were found to function in both defense- and senescence-related pathways in Arabidopsis, such as the transcription factor *WRKY53* (Jiao et al., 2022), the cell wall-associated kinase *WAKL10* (Li et al., 2021) or the mildew resistance locus O *MLO3* (Kusch et al., 2019). As a developmental process, senescence usually overlaps with the reproductive phase to maximize plant fitness (Gregesen et al., 2013; Kim et al., 2020). Therefore, it is possible that senescence and flowering share similar regulatory mechanisms, and leaf senescence can be triggered by floral transition. Several common regulators of senescence and flowering have been identified, such as the aging regulator *WRKY53* (Miao et al., 2004) or the clock regulator *ELF4* (Kim et al., 2018; Zhang et al., 2018). Additionally, both senescence and flowering were found to be affected by growth temperature (Wingler, 2011). My obtained results further

consolidated this observation, as senescence was tightly associated with temperature and flowering-related traits in the correlation test (**Figure 6**).

GWA studies are conducted to scan the whole genome using case-control samples for the responsible loci of the phenotype of interest. The pleiotropic characteristic of senescence suggests that a model combining multiple relevant phenotypic traits for loci search would likely be more powerful compared to the single trait-based models (Yang et al., 2016). Furthermore, pleiotropic genes tend to play primary roles in the functional pathways and can provide insights into the shared underlying biology (Solovieff et al., 2013). Employing PC analysis is useful in studying the causal relationship between the genetic and phenotypic variations among individuals or cultivars of the same species. My GWA analysis has successfully identified *ACD6* as a regulator of leaf senescence in Arabidopsis natural accessions (**Figure 7**). Consistently, a study employing the QTL approach also found that *ACD6* regulates leaf senescence, rosette growth, leaf chlorophyll content, as well as leaf nitrogen and carbon percentages (Jasinski et al., 2021).

QTL mapping has been proven to be a powerful method for discovering genetic loci responsible for a given trait in F2 or RIL populations. The genetic basis of the senescence pathway in Arabidopsis has been studied using this approach (reviewed in Kim et al., 2018). However, QTL mapping also comes with two major drawbacks regarding allelic diversity and mapping resolution (reviewed in Korte and Farlow, 2013). Furthermore, the lab populations in general will differ in allele frequencies and combinations compared to those in the natural population (Weigei, 2012), which limits the functional investigation of the natural phenotypic variations. My approach using

GWA analysis can overcome the aforementioned limitations, thus providing a more comprehensive view of the functional diversity present within Arabidopsis natural accessions. Interestingly, among the major PC values that have been used for GWA analysis, only PC2 successfully identified a genetic locus with significant association (**Figure 7**). A previous study has indicated the importance of PC values that explain a small amount of total variance. This is primarily due to the fact that many genetic variants with opposite effects on positively correlated traits are exclusively associated with a single or a few traits (Aschard et al., 2014). This study also proposed a new approach that combines signals across all PCs for GWA analysis, which was shown to significantly enhance the power of the model compared to the conventional approach. This combined PC strategy may be useful to identify candidate markers in genetic association tests and should be considered in future senescence studies.

ACD6 encodes a transmembrane protein with an N-terminal ankyrin repeat domain (Lu et al., 2005). The ankyrin domain is one of the most common protein motifs in nature comprising 30-34 amino acid residues that mediate protein-protein interactions (Li et al., 2006). ACD6 has recently been identified as a transmembrane ion chanel that modulate calcium influx (Chen et al., 2023). This ankyrin protein was found to be involved in plant biotic and abiotic stress responses as a regulator of SA signaling pathway (Todesco et al., 2014, Pluharova et al., 2019). SA was found to be involved in age-induced but not dark-induced leaf senescence (Buchanan-Wollaston et al., 2005). As an important regulator in the SA signaling pathway, ACD6 may function exclusively in age-induced leaf senescence. My obtained results have confirmed this speculation, as knocking out ACD6 only delayed the plant senescence

responses under normal growth conditions (**Figure 11**, **Figure 12**). Previous studies indicated that *ACD6* is specifically expressed in leaf tissues over the entire leaf lifespan in an age-dependent manner (eFP Browser, Winter et al., 2007; Andriankaja et al., 2012; Woo et al., 2016). Furthermore, *ACD6* expression are both SA- and light-dependent (Lu et al., 2003). The dark treatment possibly suppresses the *ACD6* transcript level, resulting in similar responses between Col-0 and the two examined *acd6-KO* mutants (**Figure 12**).

Arabidopsis natural accessions display high levels of variations in both genotypes and phenotypes (Shindo et al., 2007). My obtained results indicated that the functional activities of *ACD6* in age-induced leaf senescence are accession-dependent (**Figure 14**, **Figure 15**). Loss-of-function mutations of *ACD6* in the early senescence accessions Mz-0 and Est-1 significantly delayed age-induced leaf senescence responses in all examined molecular and physiological parameters but showed negligible effects in the delayed senescence accessions Bur-0 and Kin-0 (**Figure 14**, **Figure 15**). This implies that *ACD6* may have potentially adaptive roles, and the genetic variations of *ACD6* might be responsible for the different senescence responses among Arabidopsis accessions. The *ACD6* locus was found to feature extensive sequence variation in wild populations with clear functional differences. The hyperactive *ACD6* allele, which was first identified from Est-1 accession, functions in defense pathways against a wide range of pathogens (Todesco et al., 2010). These observations further indicate the crosstalk between developmental leaf senescence and defense, and *ACD6* may be an important intersection that links these two pathways.

The accession-dependent activities of *ACD6* were further confirmed in the SA-induced senescence treatment, connecting the age-induced leaf senescence with SA-related pathways (**Figure 18**, **Figure 19**, **Figure 20**). *ACD6* and SA were found to mutually affect each other in many aspects. For example, SA is required for *ACD6* expressions, and knocking out *ACD6* results in reduced endogenous SA accumulation (Lu et al., 2003). The gain-of-function mutant *acd6-1* displayed increased responsiveness to SA (Rate et al., 1999). SA has been tightly associated with plant defense against various biotic and abiotic stress factors (Mohamed et al., 2020; Song et al., 2023). Furthermore, SA pathway was found to function exclusively in age-induced but not dark-induced leaf senescence (Buchanan-Wollaston et al., 2005). Given the correlation between age-induced leaf senescence and various environmental and physiological factors such as humidity, temperature or defense (**Figure 6**) along with the functional specificity of *ACD6* in age-induced leaf senescence (**Figure 11**, **Figure 14**), the involvement of SA-related pathways to senescence *via ACD6* is comprehensible. It is also noteworthy that the SA-induced senescence responses from the examined accessions are different from their respective age-induced senescence phenotypes (**Figure 14**, **Figure 18**). One possible explanation for this observation is the effects of artificial starvation caused by the detached leaves system, which can vary among natural accessions as indicated in previous studies (Bedu et al., 2020; Ikram et al., 2012). The *in planta* SA-induced senescence assay can provide more insights regarding the functional roles of *ACD6* in SA-related and age-induced senescence pathways.

III. CONCLUSION

This study has provided further insights into the regulatory mechanisms of leaf senescence in Arabidopsis natural accessions. By employing the phenome high-throughput investigator, I was able to comprehensively evaluate senescence responses among 234 Arabidopsis natural accessions. I also successfully identified various environmental and physiological factors that highly affect senescence phenotypes. The obtained results indicate the differences between age- and dark-induced leaf senescence, which may be useful for optimizing future studies on senescence biology. The variations of senescence among Arabidopsis natural populations was found to be regulated by the *ACCELERATED CELL DEATH 6* (*ACD6*) locus. The accessions-dependent activities of *ACD6* highlighted the adaptation process of Arabidopsis via evolution. Furthermore, *ACD6* may serve as an important integrator linking between age-induced leaf senescence and salicylic acid signaling pathways.

References

Andriankaja, M., Dhondt, S., De Bodt, S., Vanhaeren, H., Coppens, F., De Milde, L., ... & Inzé, D. (2012). Exit from proliferation during leaf development in Arabidopsis thaliana: a not-so-gradual process. Developmental cell, 22(1), 64-78.

Aschard, H., Vilhjálmsson, B. J., Greliche, N., Morange, P. E., Trégouët, D. A., & Kraft, P. (2014). Maximizing the power of principal-component analysis of correlated phenotypes in genome-wide association studies. The American Journal of Human Genetics, 94(5), 662-676.

Atwell, S., Huang, Y. S., Vilhjálmsson, B. J., Willems, G., Horton, M., Li, Y., ... & Nordborg, M. (2010). Genome-wide association study of 107 phenotypes in Arabidopsis thaliana inbred lines. Nature, 465(7298), 627-631.

Avila-Ospina, L., Moison, M., Yoshimoto, K., & Masclaux-Daubresse, C. (2014). Autophagy, plant senescence, and nutrient recycling. Journal of Experimental Botany, 65(14), 3799-3811.

Bedu, M., Marmagne, A., Masclaux-Daubresse, C., & Chardon, F. (2020). Transcriptional plasticity of autophagy-related genes correlates with the genetic response to nitrate starvation in Arabidopsis thaliana. Cells, 9(4), 1021.

Breeze, E., Harrison, E., McHattie, S., Hughes, L., Hickman, R., Hill, C., ... & Buchanan-Wollaston, V. (2011). High-resolution temporal profiling of transcripts during Arabidopsis leaf senescence reveals a distinct chronology of processes and regulation. The Plant Cell, 23(3), 873-894.

Buchanan-Wollaston, V., Page, T., Harrison, E., Breeze, E., Lim, P. O., Nam, H. G., ... & Leaver, C. J. (2005). Comparative transcriptome analysis reveals significant differences in gene expression and signalling pathways between developmental and dark/starvation-induced senescence in Arabidopsis. The Plant Journal, 42(4), 567-585.

Chen, J., Li, L., Kim, J. H., Neuhäuser, B., Wang, M., Thelen, M., ... & Zhu, W. (2023). Small proteins modulate ion-channel-like ACD6 to regulate immunity in Arabidopsis thaliana. Molecular Cell.

Clough, S. J., & Bent, A. F. (1998). Floral dip: a simplified method for Agrobacterium-mediated transformation of Arabidopsis thaliana. The plant journal, 16(6), 735-743.

Collyer, M. L., Sekora, D. J., & Adams, D. C. (2015). A method for analysis of phenotypic change for phenotypes described by high-dimensional data. Heredity, 115(4), 357-365.

Girondé, A., Poret, M., Etienne, P., Trouverie, J., Bouchereau, A., Le Cahérec, F., ... & Avice, J. C. (2015). A comparative study of proteolytic mechanisms during leaf senescence of four genotypes of winter oilseed rape highlighted relevant physiological and molecular traits for NRE improvement. Plants, 5(1), 1.

Goddard, M. E., Kemper, K. E., MacLeod, I. M., Chamberlain, A. J., & Hayes, B. J. (2016). Genetics of complex traits: prediction of phenotype, identification of causal polymorphisms and genetic architecture. Proceedings of the Royal Society B: Biological Sciences, 283(1835), 20160569.

Gregersen, P. L., Culetic, A., Boschian, L., & Krupinska, K. (2013). Plant senescence and crop productivity. Plant molecular biology, 82, 603-622.

Grimm, D. G., Roqueiro, D., Salomé, P. A., Kleeberger, S., Greshake, B., Zhu, W., ... & Borgwardt, K. M. (2017). easyGWAS: a cloud-based platform for comparing the results of genome-wide association studies. The Plant Cell, 29(1), 5-19.

Guo, Y., & Gan, S. (2006). AtNAP, a NAC family transcription factor, has an important role in leaf senescence. The Plant Journal, 46(4), 601-612.

Guo, Y., & Gan, S. S. (2012). Convergence and divergence in gene expression profiles induced by leaf senescence and 27 senescence-promoting hormonal, pathological and environmental stress treatments. Plant, Cell & Environment, 35(3), 644-655.

He, L., Wu, W., Zinta, G., Yang, L., Wang, D., Liu, R., ... & Zhu, J. K. (2018). A naturally occurring epiallele associates with leaf senescence and local climate adaptation in Arabidopsis accessions. Nature communications, 9(1), 460.

Hörtensteiner, S., & Feller, U. (2002). Nitrogen metabolism and remobilization during senescence. Journal of experimental botany, 53(370), 927-937.

Horton, M. W., Hancock, A. M., Huang, Y. S., Toomajian, C., Atwell, S., Auton, A., ... & Bergelson, J. (2012). Genome-wide patterns of genetic variation in worldwide

Arabidopsis thaliana accessions from the RegMap panel. Nature genetics, 44(2), 212-216.

Ikram, S., Bedu, M., Daniel-Vedele, F., Chaillou, S., & Chardon, F. (2012). Natural variation of Arabidopsis response to nitrogen availability. Journal of Experimental Botany, 63(1), 91-105.

Jasinski, S., Fabrissin, I., Masson, A., Marmagne, A., Lécureuil, A., Bill, L., & Chardon, F. (2021). ACCELERATED CELL DEATH 6 acts on natural leaf senescence and nitrogen fluxes in Arabidopsis. Frontiers in Plant Science, 11, 611170.

Jiao, C., Li, K., Zuo, Y., Gong, J., Guo, Z., & Shen, Y. (2022). CALMODULIN1 and WRKY53 function in plant defense by negatively regulating the jasmonic acid biosynthesis pathway in Arabidopsis. International Journal of Molecular Sciences, 23(14), 7718.

Kim, J. H., Woo, H. R., Kim, J., Lim, P. O., Lee, I. C., Choi, S. H., ... & Nam, H. G. (2009). Trifurcate feed-forward regulation of age-dependent cell death involving miR164 in Arabidopsis. Science, 323(5917), 1053-1057.

Kim, H. J., Park, J. H., Kim, J., Kim, J. J., Hong, S., Kim, J., ... & Hwang, D. (2018). Time-evolving genetic networks reveal a NAC troika that negatively regulates leaf senescence in Arabidopsis. Proceedings of the National Academy of Sciences, 115(21), E4930-E4939.

Kim, H., Kim, H. J., Vu, Q. T., Jung, S., McClung, C. R., Hong, S., & Nam, H. G. (2018). Circadian control of ORE1 by PRR9 positively regulates leaf senescence in Arabidopsis. Proceedings of the National Academy of Sciences, 115(33), 8448-8453.

Kim, J., Kim, J. H., Lyu, J. I., Woo, H. R., & Lim, P. O. (2018). New insights into the regulation of leaf senescence in Arabidopsis. Journal of Experimental Botany, 69(4), 787-799.

Kim, H., Park, S. J., Kim, Y., & Nam, H. G. (2020). Subcellular localization of GIGANTEA regulates the timing of leaf senescence and flowering in Arabidopsis. Frontiers in Plant Science, 11, 589707.

Korte, A., & Farlow, A. (2013). The advantages and limitations of trait analysis with GWAS: a review. Plant methods, 9(1), 1-9.

Koyama, T. (2018). A hidden link between leaf development and senescence. Plant Science, 276, 105-110.

Kusch, S., Thiery, S., Reinstädler, A., Gruner, K., Zienkiewicz, K., Feussner, I., & Panstruga, R. (2019). Arabidopsis mlo3 mutant plants exhibit spontaneous callose deposition and signs of early leaf senescence. Plant molecular biology, 101, 21-40.

Levey, S., & Wingler, A. (2005). Natural variation in the regulation of leaf senescence and relation to other traits in Arabidopsis. Plant, Cell & Environment, 28(2), 223-231.

Li, J., Mahajan, A., & Tsai, M. D. (2006). Ankyrin repeat: a unique motif mediating protein− protein interactions. Biochemistry, 45(51), 15168-15178.

Li, L., Li, K., Ali, A., & Guo, Y. (2021). AtWAKL10, a cell wall associated receptor-like kinase, negatively regulates leaf senescence in Arabidopsis thaliana. International Journal of Molecular Sciences, 22(9), 4885.

Lim, P. O., Woo, H. R., & Nam, H. G. (2003). Molecular genetics of leaf senescence in Arabidopsis. Trends in plant science, 8(6), 272-278.

Lim, P. O., Kim, H. J., & Gil Nam, H. (2007). Leaf senescence. Annu. Rev. Plant Biol., 58, 115-136.

Lu, H., Rate, D. N., Song, J. T., & Greenberg, J. T. (2003). ACD6, a novel ankyrin protein, is a regulator and an effector of salicylic acid signaling in the Arabidopsis defense response. The Plant Cell, 15(10), 2408-2420.

Lu, H., Liu, Y., & Greenberg, J. T. (2005). Structure–function analysis of the plasma membrane-localized Arabidopsis defense component ACD6. The Plant Journal, 44(5), 798-809.

Luquez, V. M., Sasal, Y., Medrano, M., Martín, M. I., Mujica, M., & Guiamét, J. J. (2006). Quantitative trait loci analysis of leaf and plant longevity in Arabidopsis thaliana. Journal of Experimental Botany, 57(6), 1363-1372.

Lyu, J. I., Baek, S. H., Jung, S., Chu, H., Nam, H. G., Kim, J., & Lim, P. O. (2017). High-throughput and computational study of leaf senescence through a phenomic approach. Frontiers in Plant Science, 8, 250.

Lyu, J. I., Kim, J. H., Chu, H., Taylor, M. A., Jung, S., Baek, S. H., ... & Kim, J. (2019). Natural allelic variation of GVS 1 confers diversity in the regulation of leaf senescence in Arabidopsis. New Phytologist, 221(4), 2320-2334.

Miao, Y., Laun, T., Zimmermann, P., & Zentgraf, U. (2004). Targets of the WRKY53 transcription factor and its role during leaf senescence in Arabidopsis. Plant molecular biology, 55, 853-867.

Mohamed, H. I., El-Shazly, H. H., & Badr, A. (2020). Role of salicylic acid in biotic and abiotic stress tolerance in plants. Plant Phenolics in Sustainable Agriculture: Volume 1, 533-554.

Pluhařová, K., Leontovyčová, H., Stoudková, V., Pospíchalová, R., Maršík, P., Klouček, P., ... & Kalachova, T. (2019). “Salicylic acid mutant collection” as a tool to explore the role of salicylic acid in regulation of plant growth under a changing environment. International Journal of Molecular Sciences, 20(24), 6365.

Rate, D. N., Cuenca, J. V., Bowman, G. R., Guttman, D. S., & Greenberg, J. T. (1999). The gain-of-function Arabidopsis acd6 mutant reveals novel regulation and function of the salicylic acid signaling pathway in controlling cell death, defenses, and cell growth. The Plant Cell, 11(9), 1695-1708.

Roach, D. A. (1994). Evolutionary senescence in plants. Genetics and evolution of aging, 71-82.

Scarpeci, T. E., Frea, V. S., Zanor, M. I., & Valle, E. M. (2017). Overexpression of AtERF019 delays plant growth and senescence, and improves drought tolerance in Arabidopsis. Journal of experimental botany, 68(3), 673-685.

Schippers, J. H., Jing, H. C., Hille, J., & Dijkwel, P. P. (2007). Developmental and hormonal control of leaf senescence. Senescence processes in plants, 26, 145-170.

Shindo, C., Bernasconi, G., & Hardtke, C. S. (2007). Natural genetic variation in Arabidopsis: tools, traits and prospects for evolutionary ecology. Annals of Botany, 99(6), 1043-1054.

Solovieff, N., Cotsapas, C., Lee, P. H., Purcell, S. M., & Smoller, J. W. (2013). Pleiotropy in complex traits: challenges and strategies. Nature Reviews Genetics, 14(7), 483-495.

Song, W., Shao, H., Zheng, A., Zhao, L., & Xu, Y. (2023). Advances in Roles of Salicylic Acid in Plant Tolerance Responses to Biotic and Abiotic Stresses. Plants, 12(19), 3475.

Thomas, H. (2013). Senescence, ageing and death of the whole plant. New Phytologist, 197(3), 696-711.

Todesco, M., Balasubramanian, S., Hu, T. T., Traw, M. B., Horton, M., Epple, P., ... & Weigel, D. (2010). Natural allelic variation underlying a major fitness trade-off in Arabidopsis thaliana. Nature, 465(7298), 632-636.

Todesco, M., Kim, S. T., Chae, E., Bomblies, K., Zaidem, M., Smith, L. M., ... & Laitinen, R. A. (2014). Activation of the Arabidopsis thaliana immune system by combinations of common ACD6 alleles. PLoS Genetics, 10(7), e1004459.

Uauy, C., Distelfeld, A., Fahima, T., Blechl, A., & Dubcovsky, J. (2006). A NAC gene regulating senescence improves grain protein, zinc, and iron content in wheat. Science, 314(5803), 1298-1301.

van der Graaff, E., Schwacke, R., Schneider, A., Desimone, M., Flugge, U. I., & Kunze, R. (2006). Transcription analysis of Arabidopsis membrane transporters and hormone pathways during developmental and induced leaf senescence. Plant physiology, 141(2), 776-792.

Wang, S., Dvorkin, D., & Da, Y. (2012). SNPEVG: a graphical tool for GWAS graphing with mouse clicks. BMC bioinformatics, 13, 1-6.

Weigel, D. (2012). Natural variation in Arabidopsis: from molecular genetics to ecological genomics. Plant physiology, 158(1), 2-22.

Weaver, L. M., & Amasino, R. M. (2001). Senescence is induced in individually darkened Arabidopsis leaves, but inhibited in whole darkened plants. Plant Physiology, 127(3), 876-886.

Wingler, A., Purdy, S. J., Edwards, S. A., Chardon, F., & Masclaux-Daubresse, C. (2010). QTL analysis for sugar-regulated leaf senescence supports flowering-dependent and-independent senescence pathways. New Phytologist, 185(2), 420-433.

Wingler, A. (2011). Interactions between flowering and senescence regulation and the influence of low temperature in Arabidopsis and crop plants. Annals of Applied Biology, 159(3), 320-338.

Winter, D., Vinegar, B., Nahal, H., Ammar, R., Wilson, G. V., & Provart, N. J. (2007). An "Electronic Fluorescent Pictograph" browser for exploring and analyzing large-scale biological data sets. PloS one, 2(8), e718.

Woo, H. R., Chung, K. M., Park, J. H., Oh, S. A., Ahn, T., Hong, S. H., ... & Nam, H. G. (2001). ORE9, an F-box protein that regulates leaf senescence in Arabidopsis. The Plant Cell, 13(8), 1779-1790.

Woo, H. R., Koo, H. J., Kim, J., Jeong, H., Yang, J. O., Lee, I. H., ... & Lim, P. O. (2016). Programming of plant leaf senescence with temporal and inter-organellar coordination of transcriptome in Arabidopsis. Plant physiology, 171(1), 452-467.

Woo, H. R., Kim, H. J., Lim, P. O., & Nam, H. G. (2019). Leaf senescence: systems and dynamics aspects. Annual Review of Plant Biology, 70, 347-376.

Xing, H. L., Dong, L., Wang, Z. P., Zhang, H. Y., Han, C. Y., Liu, B., ... & Chen, Q. J. (2014). A CRISPR/Cas9 toolkit for multiplex genome editing in plants. BMC plant biology, 14(1), 1-12.

Yang, J. J., Li, J., Williams, L. K., & Buu, A. (2016). An efficient genome-wide association test for multivariate phenotypes based on the Fisher combination function. BMC bioinformatics, 17, 1-11.

Zhang, X., Ju, H. W., Chung, M. S., Huang, P., Ahn, S. J., & Kim, C. S. (2011). The RR-type MYB-like transcription factor, AtMYBL, is involved in promoting leaf senescence and modulates an abiotic stress response in Arabidopsis. Plant and Cell Physiology, 52(1), 138-148.

Zhang, Y., Wang, Y., Wei, H., Li, N., Tian, W., Chong, K., & Wang, L. (2018). Circadian evening complex represses jasmonate-induced leaf senescence in Arabidopsis. Molecular Plant, 11(2), 326-337.

Zhang, Y. M., Guo, P., Xia, X., Guo, H., & Li, Z. (2021). Multiple layers of regulation on leaf senescence: New advances and perspectives. Frontiers in Plant Science, 12, 788996.

애기장대 연령 유도된 및 살리실산 유도된 잎 노화의 다양성을 조절하는 *ACCERLATED CELL DEATH 6*의 기능 연구

초록

잎의 노화는 자연환경 속에서 식물의 적응력을 높이기 위한 필수적이며 진화적으로 보존된 과정이다. 잎의 노화는 나이가 들었을 때, 광합성을 통한 에너지 생성과 축적된 고분자 물질의 분해를 통한 에너지 생성 간의 밸런스를 조절하여 식물의 서식지 적응력을 높입니다. 노화의 시작과 진행은 유전적 및 환경적 요소 간의 상호작용에 의해 결정되며, 식물의 자연 서식지 내 적응에 있어 주요 요인으로 작용한다. 본 연구에서는 애기장대(Arabidopsis)의 자연 야생형 모집단에 연령 노화의 다양성을 유발하는 유전적 기전을 이해하는 것을 목표하였다. 이를 위해 234 개의 애기장대 야생형을 대상으로 고속 표현형 분석 시스템을 활용하여 잎의 노화 반응을 종합적이며 정량적으로 분석하였다. 이를 활용하여, 노화 형질과 연관된 환경 및 생리적 요소를 확인하였다. 전장 유전체 연관 지도 분석 (GWAS)을 통해 자연 잎 노화의 다양성을 유발할 수 있는 유전변이로 *ACCELERATED CELL DEATH 6* (*ACD6*)를 발굴하였다. 조기 또는 늦은 노화 형질을 가진 자연 야생형에서 *ACD6* 를 제거하면 연령 유도 노화의 지연 정도가 다르게 나타나며, 이는 잎 연령 노화에서의 *ACD6* 의 기능이 야생형별로 다르게 작용한다는 것을 의미한다. 더 나아가, *ACD6* 이 살리실산 신호 전달 경로를 통해 잎 노화의 다양성을 조절하는 것을 확인하였다. 이를 통해 본 연구는 애기장대 자연 야생형 모집단에서의 잎 노화의 다양성을 제어하는

유전적, 환경적, 생리적 이해를 제공하며, ACD6 를 통해 작물에서의 환경 적응력 및 생존을 향상시킬 수 있을 것으로 기대된다.

Acknowledgement

First of all, I would like to express my appreciation to my professor Jeongsik Kim enthusiastically support my thesis. for his invaluable patience and feedback. Without his knowledge and expertise, this thesis project could not have completed. I also want to thank Dr. Jin Hee Kim for her generous supports and advices in the past two years. I am also grateful for my defense comittee, who have provided precious comments and suggestion to improved my study.

I am also grateful to my labmates for alway having my back without any hesitations. A special thank to my Vietnamese friends for their endless mental supports throughout my study. I could have not completed this study without their help.

Lastly, I would be remiss in not mentioning my family, especially my parents and my sister. Their belief in me has kept my spirits and motivation high during this process.